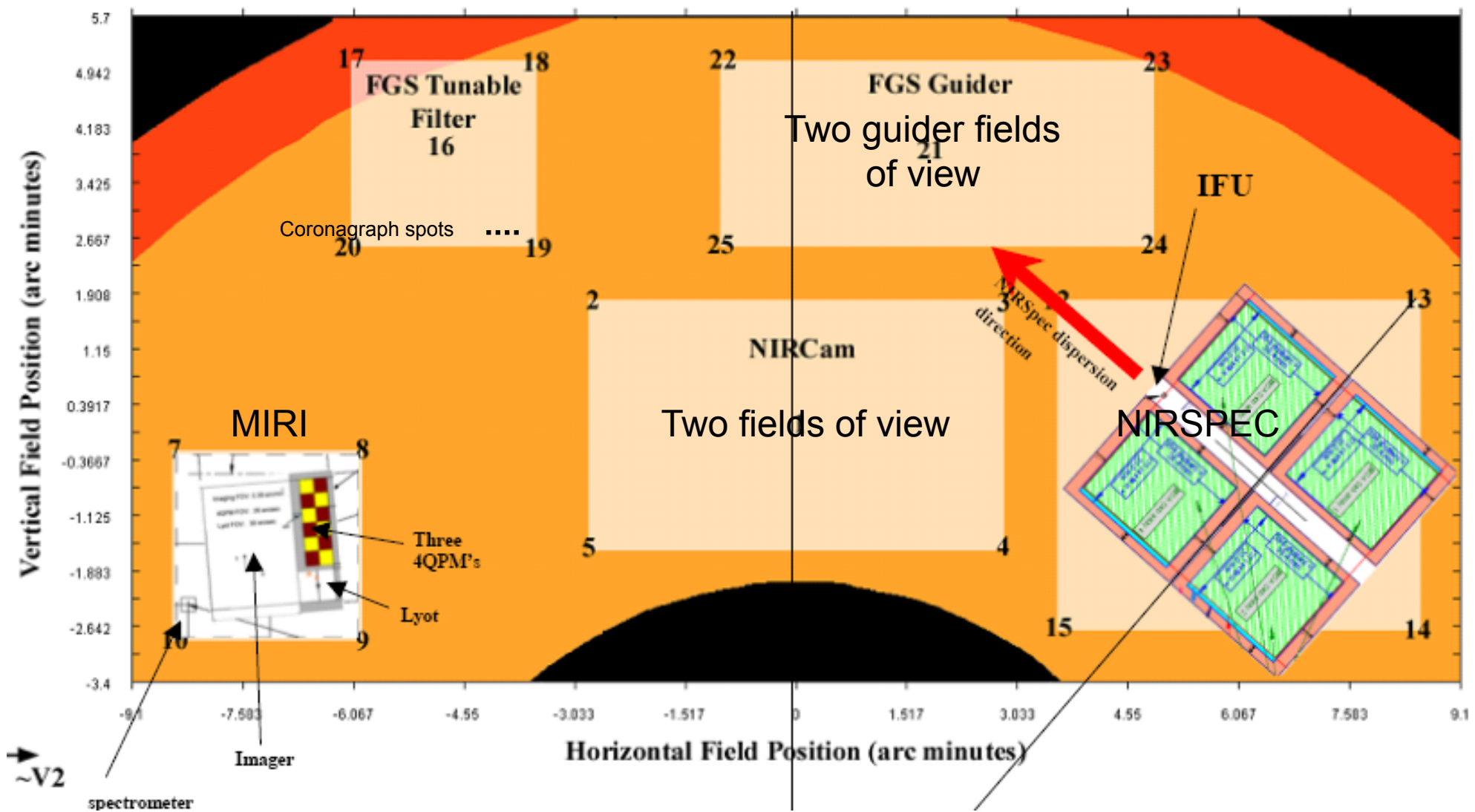




FGS/TFI instruments



- Two redundant guider fields
- Tunable Filter Imager (TFI) instrument
- Mounted on opposite sides of single optical bench
- Separate operations and pickoff mirrors
- Provided by CSA as JWST partner hardware contribution
- Principal contractor ComDev Ltd, Ottawa
- John Hutchings (NRC Canada) Guider PI
- Rene Doyon (U de Montreal) TFI PI

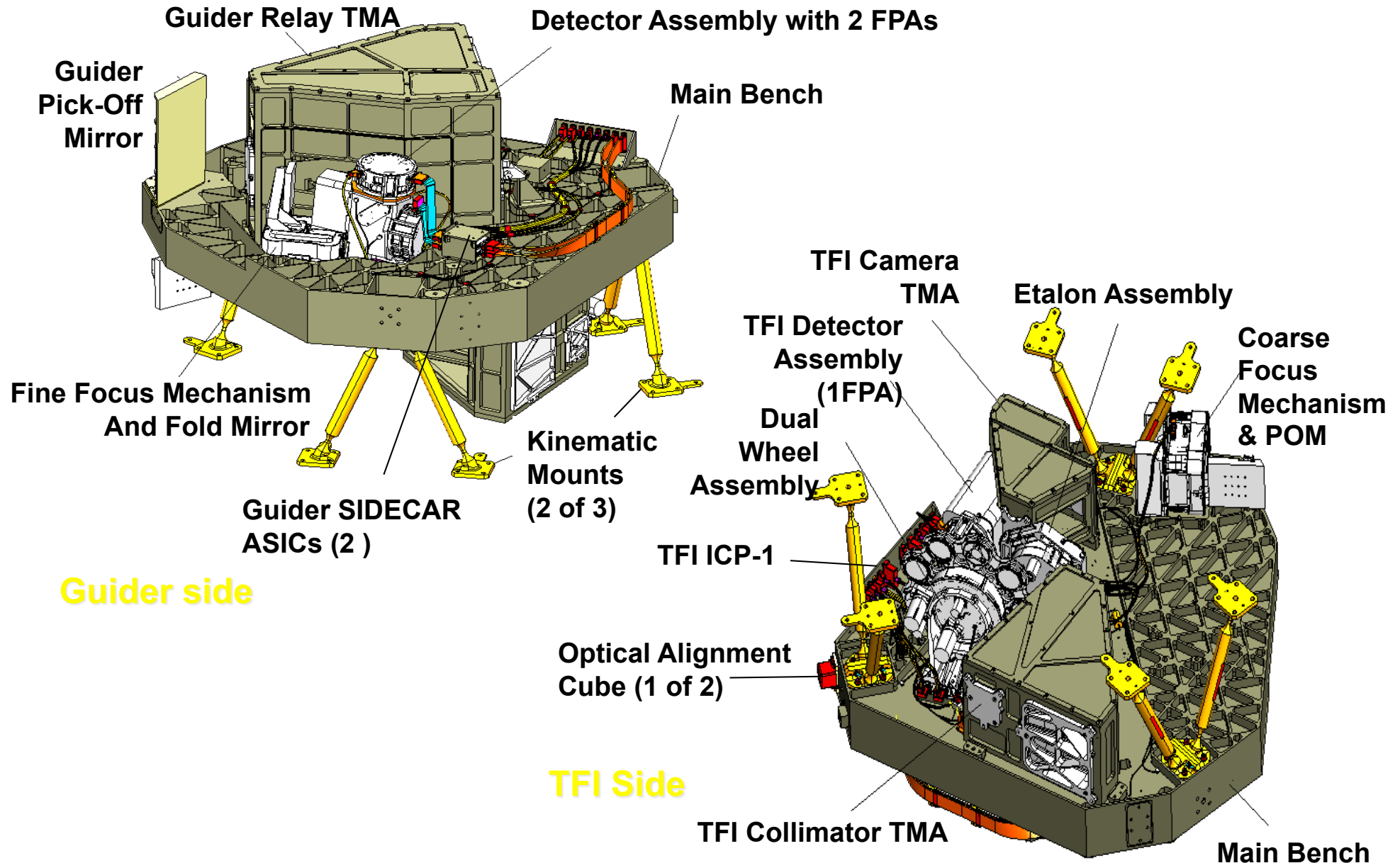




The FGS Science team



- R. Doyon (U. Montréal)
- J. Hutchings (HIA)
- R. Abraham (U of Toronto)
- L. Ferrarese (HIA)
- R. Jayawardhana (U of Toronto)
- D. Johnstone (HIA)
- D. Lafrenière (U. Montréal)
- M. Meyer (ETH, Zurich)
- J. Pipher (U. Rochester)
- M. Sawicki (St-Mary's University)
- A. Sivaramakrishnan (AMNH → STScI)





Guider



Top level requirements

- 2 Fully redundant fields of view
- Guide star position updated at 16 Hz
- Guide star centroid (NEA) 3.5mas or better
- 95% probability of GS, any place in the sky



Guider performance drivers



NEA depends on

- Guide star brightness and SED
- Optical throughput and pixel scale
- Image quality/focus
- Detector QE and read noise

Dark current not an issue – rapid reads

*All these combine to require ~5 arcmin field of view to have
95% chance of useable GS present*

No filter – all photons from 0.8 to 5 microns used

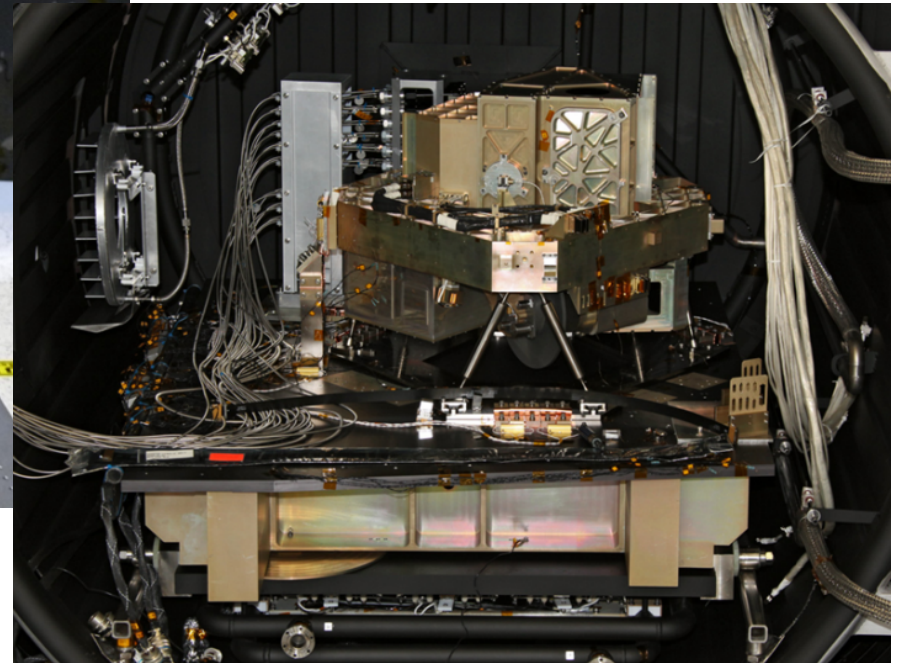
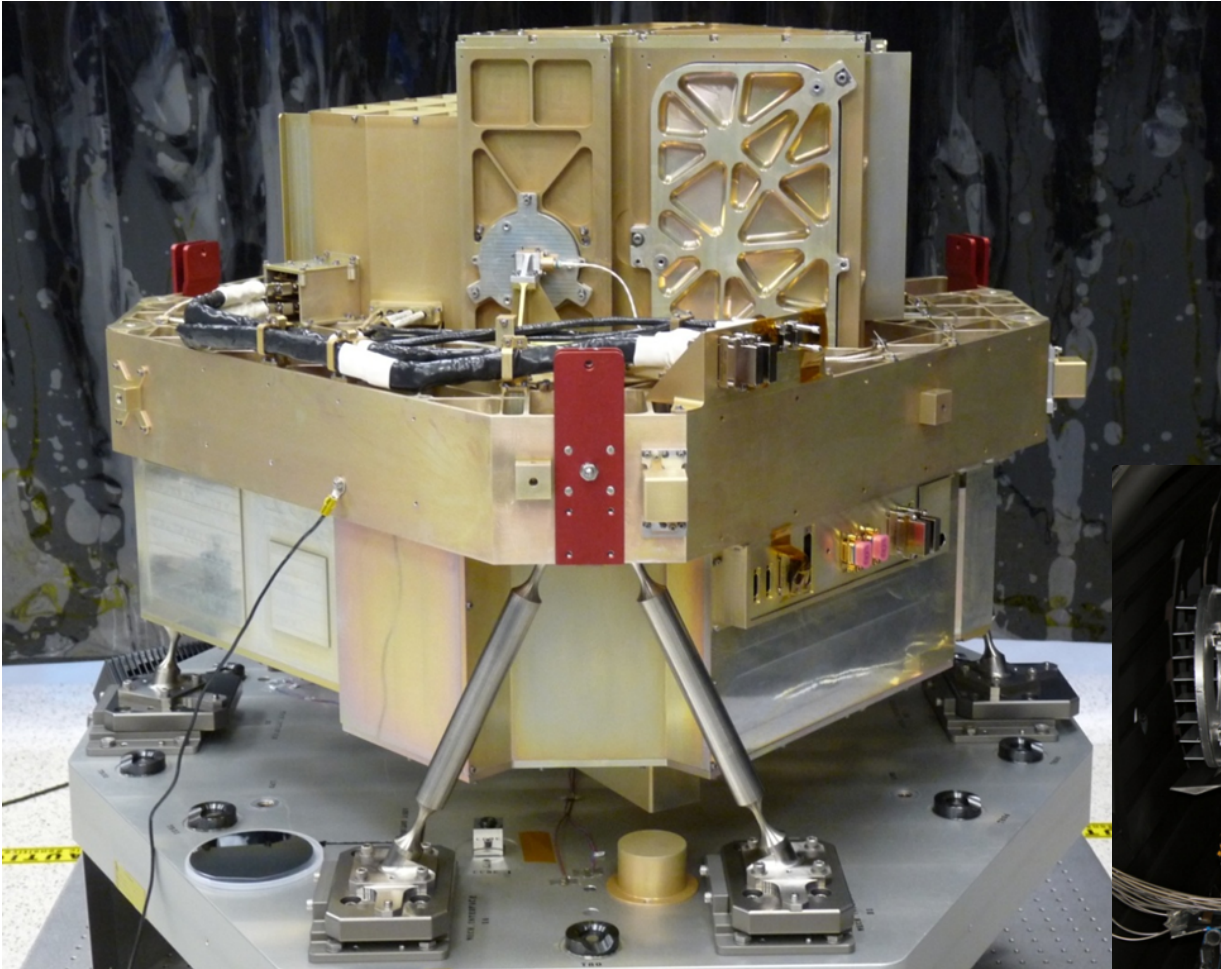


Other guider tasks



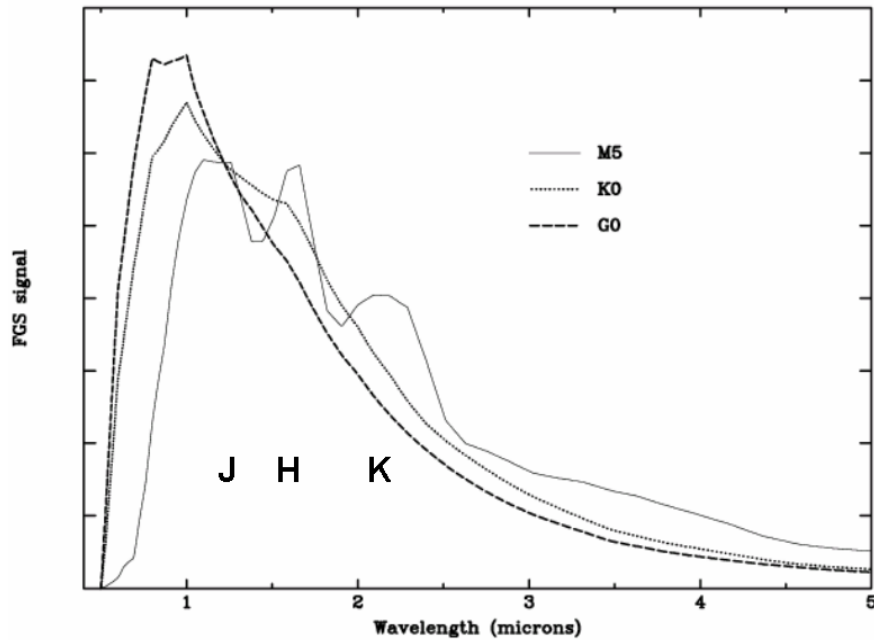
- Guiding with detector latency, dead pixels
- Target identification by pattern/brightness matching
Crowded and sparse fields, extra stars, double stars, compact galaxies
- Tracking on moving targets
9mas NEA moving up to 30mas/sec
- Guide on images during primary mirror focus, alignment, phasing
Range of image quality, flux, and focus
- Focus sweep images for wavefront sensing
Modelling images, tracking to interpret the results
- Full field imaging (science!) in non-guiding FOV
JWST's deepest images
- Calibrated boresight movement with guider/OTE focus
- Stable, known position wrt other instruments to 5mas

Fully integrated ETU

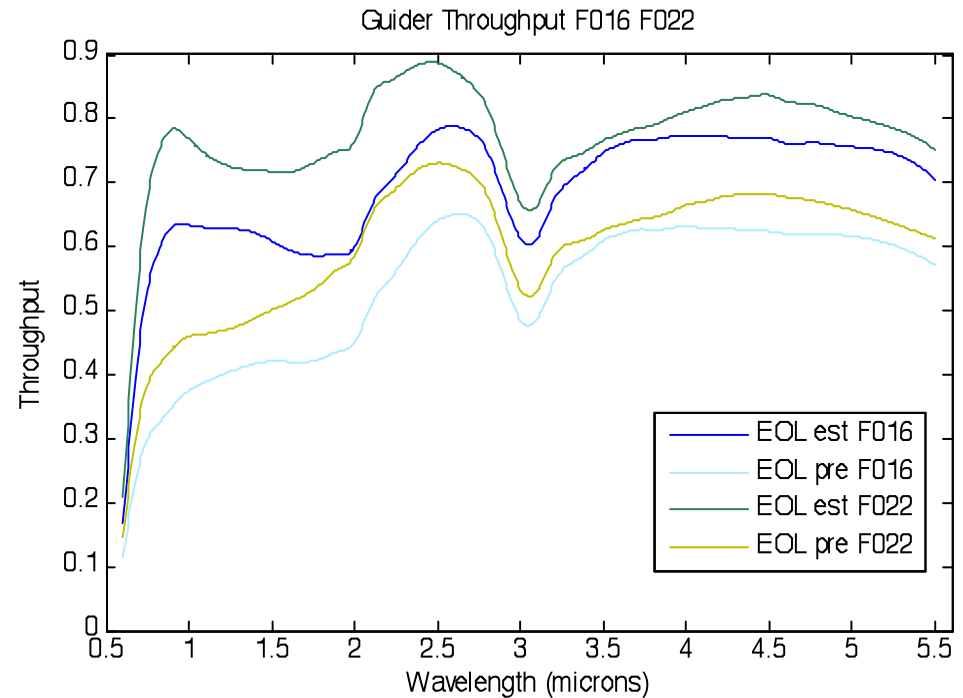




Guider signal depends on the detector selected



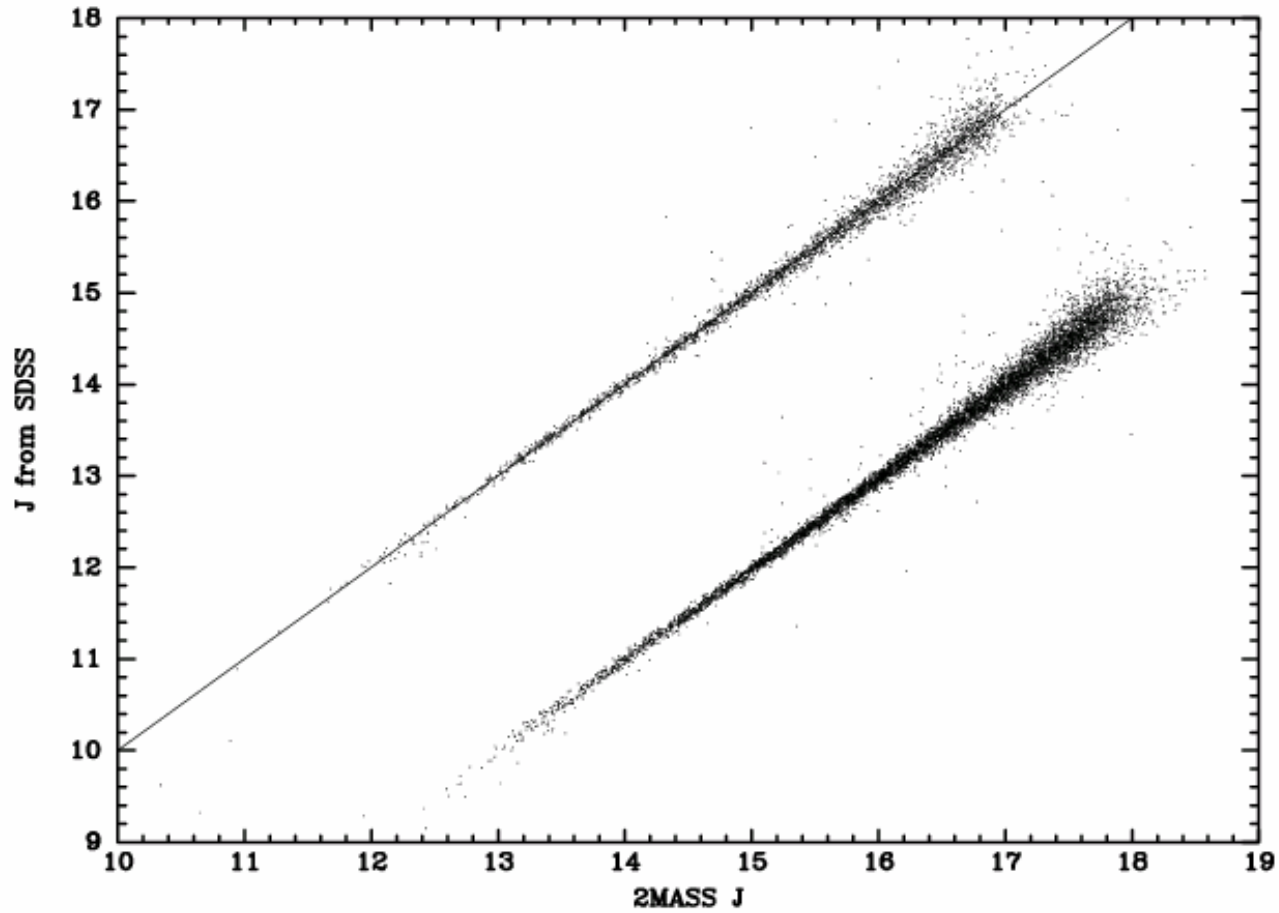
Guide star signal mostly at short wavelengths

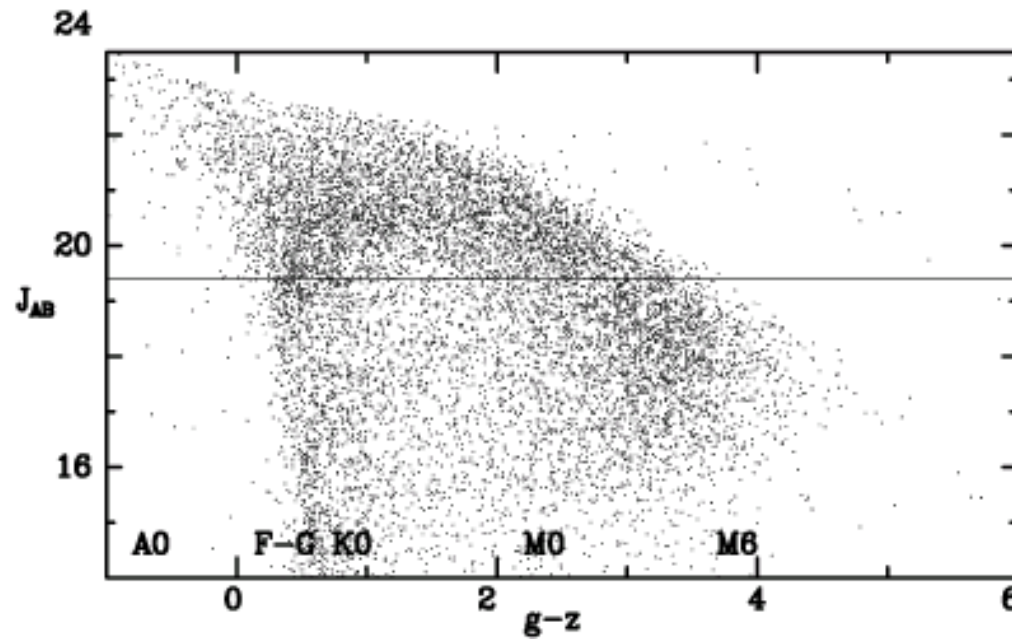


Estimates for the presently-considered PFM and flight detectors
F022 good choice for guider

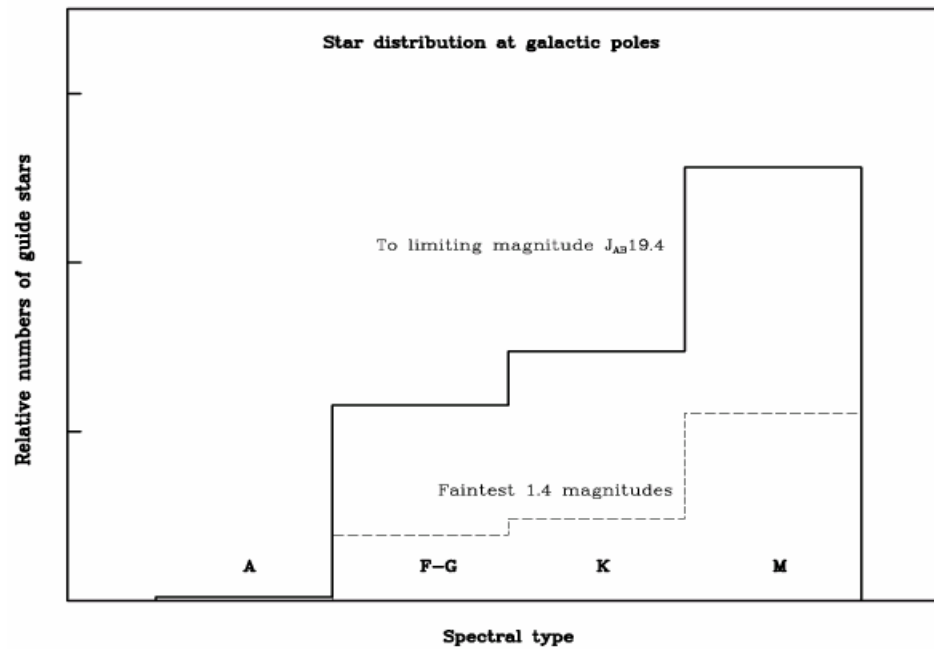


Conversion from visible to J band magnitudes





Colour distribution and number counts of guide stars at the Galactic pole



Distribution of available guide stars at Galactic pole



Available guide stars and catalogues

SDSS stars to FGS limit per single FGS field at galactic pole:	6.3
to $J_{AB} = 18.0$	3.9
10 degrees off this direction, to FGS limit	7.1

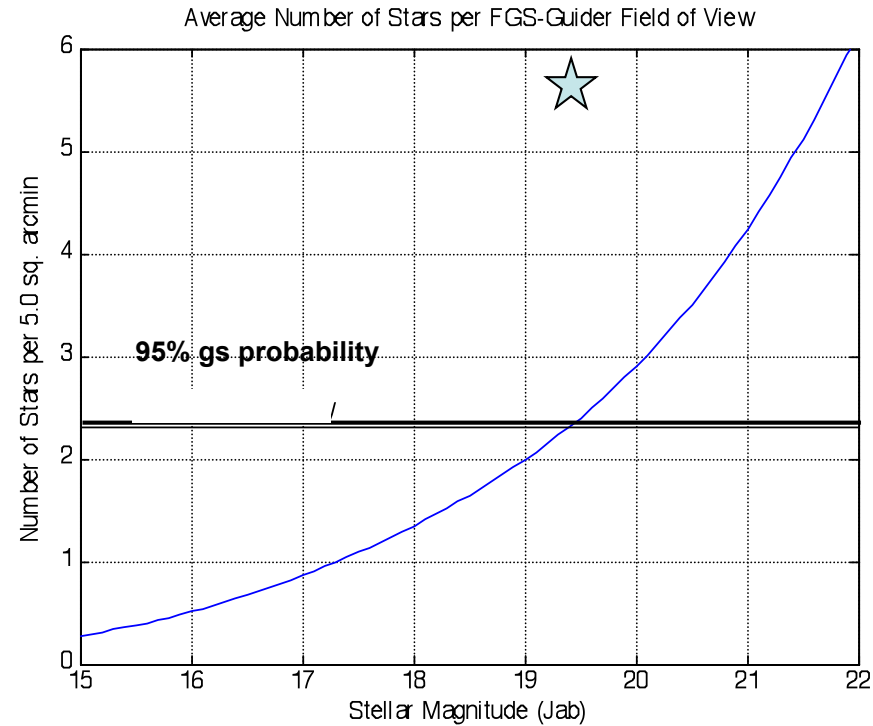
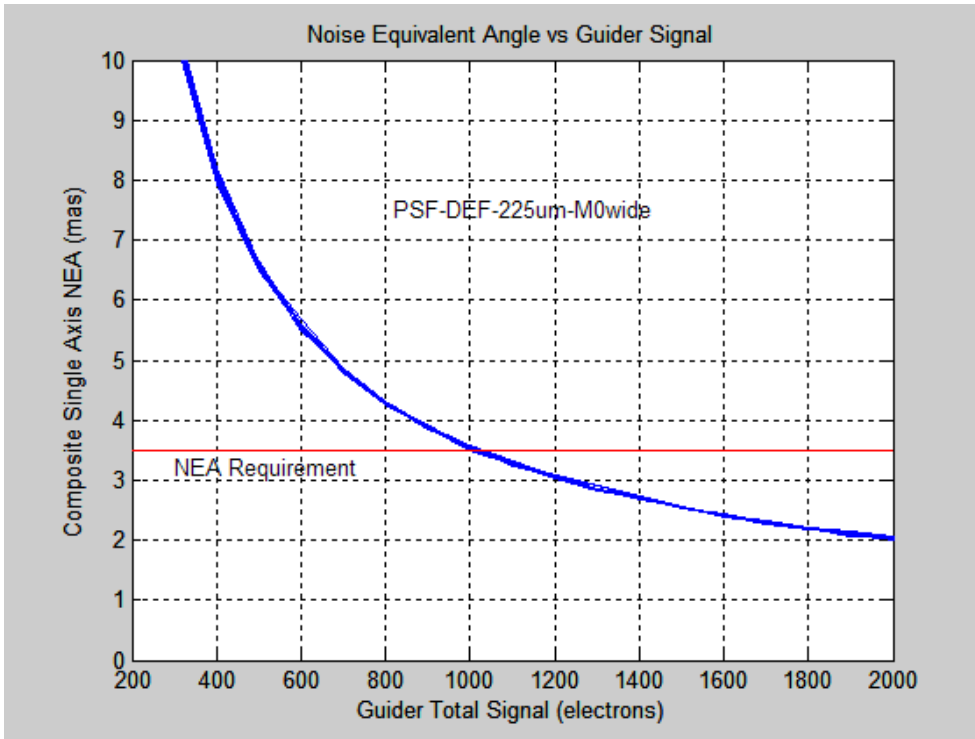
GSC2 useable stars are estimated to be 2.6 per single FGS field.
Total stars to GSC2 limit are about 10 per single FGS field at pole

FGS can guide on double stars and compact extended objects
Above SDSS numbers will likely include some of those

Need for J-band catalogue of stars near galactic poles
But need good spatial resolution: HST or ground-AO



Guide star limiting counts and magnitudes



NEA with GS signal

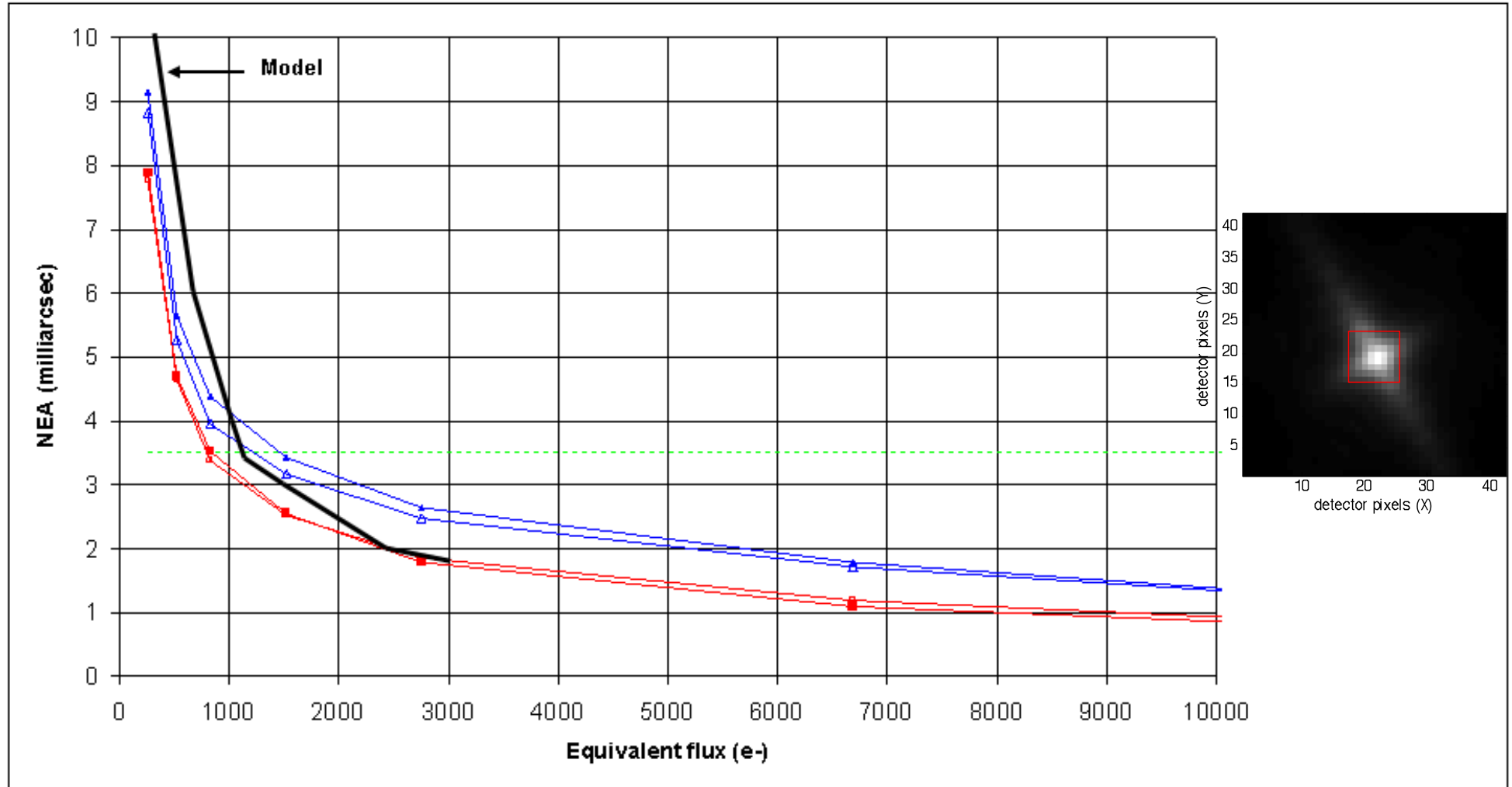
1000 counts is $J_{AB} \sim 19.4$

Read noise estimates crucial

Number of GSC2 stars per FOV

Nominal FOV is 10% larger
3 stars per field is ~95% prob

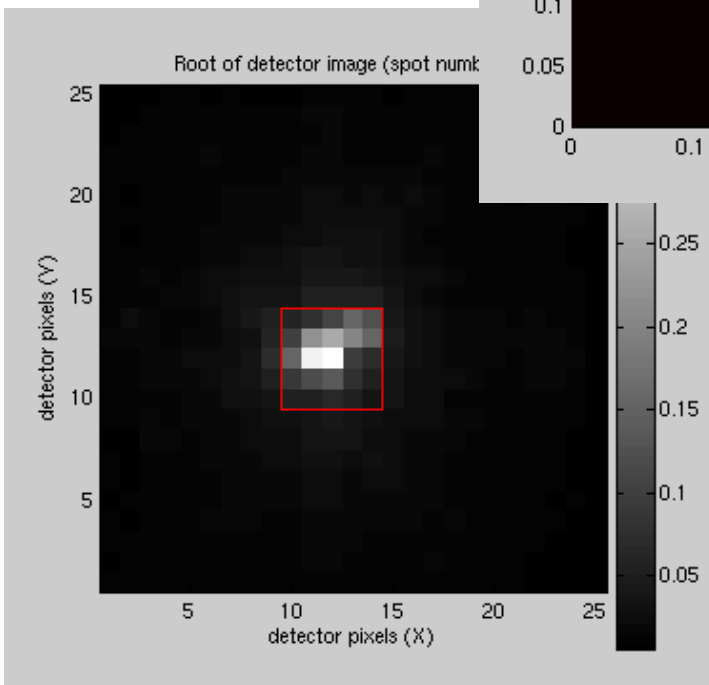
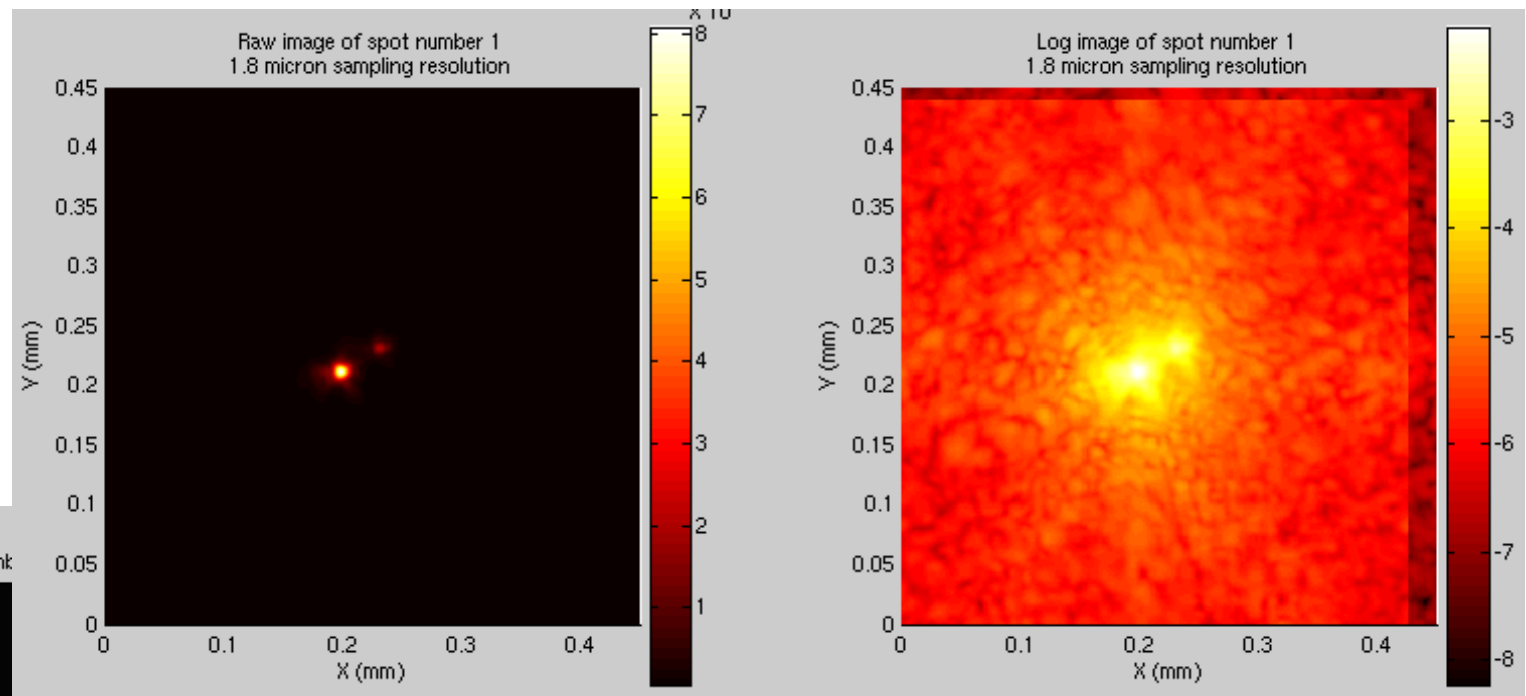
★ SDSS point sources J mag



Heavy line is model for similar centroid window and noise, flight centroid algorithm



Sep $\sim 100\text{mas}$
Flux ratio 4

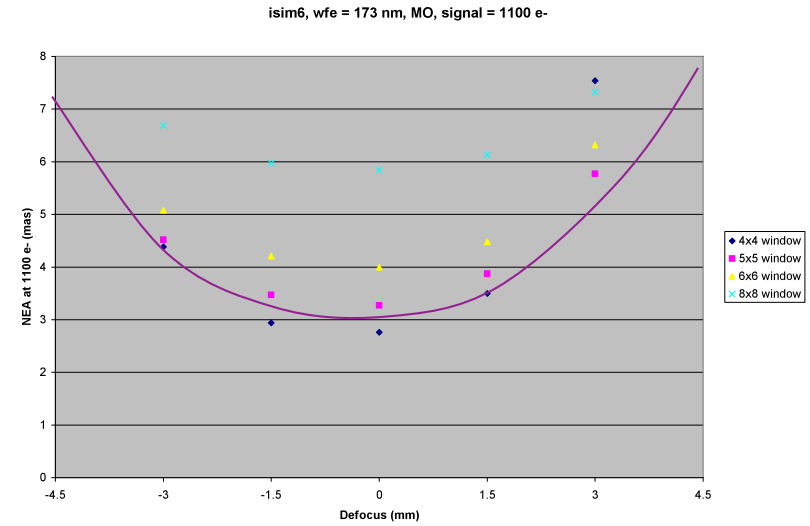
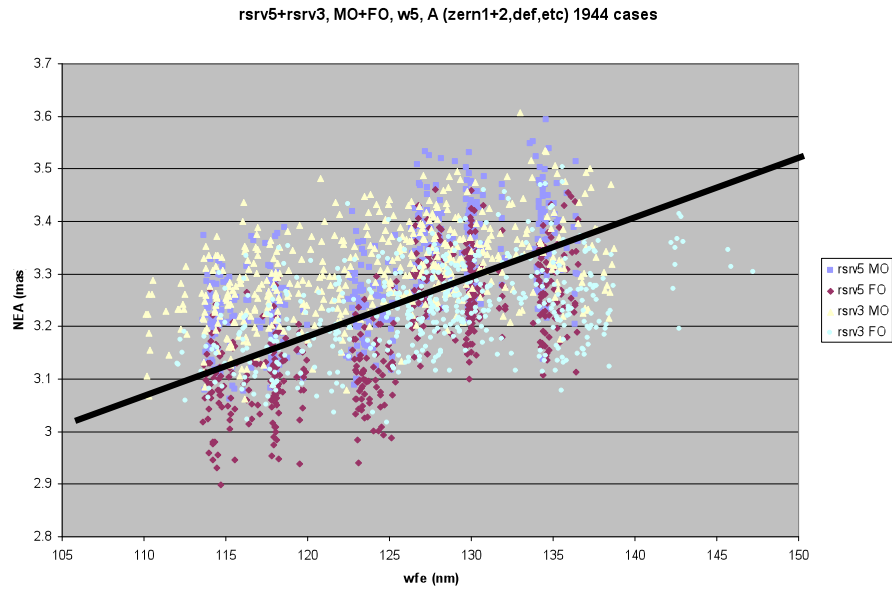


Detector pixels

*Limiting magnitude 0.7
brighter for this case*

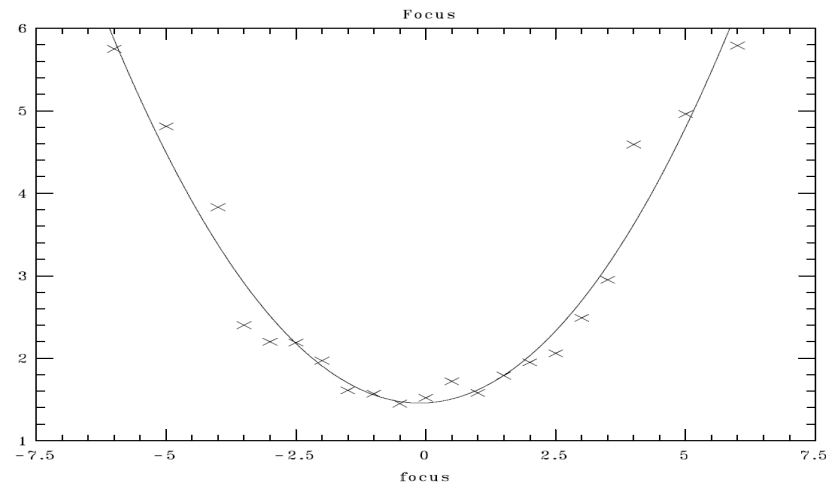


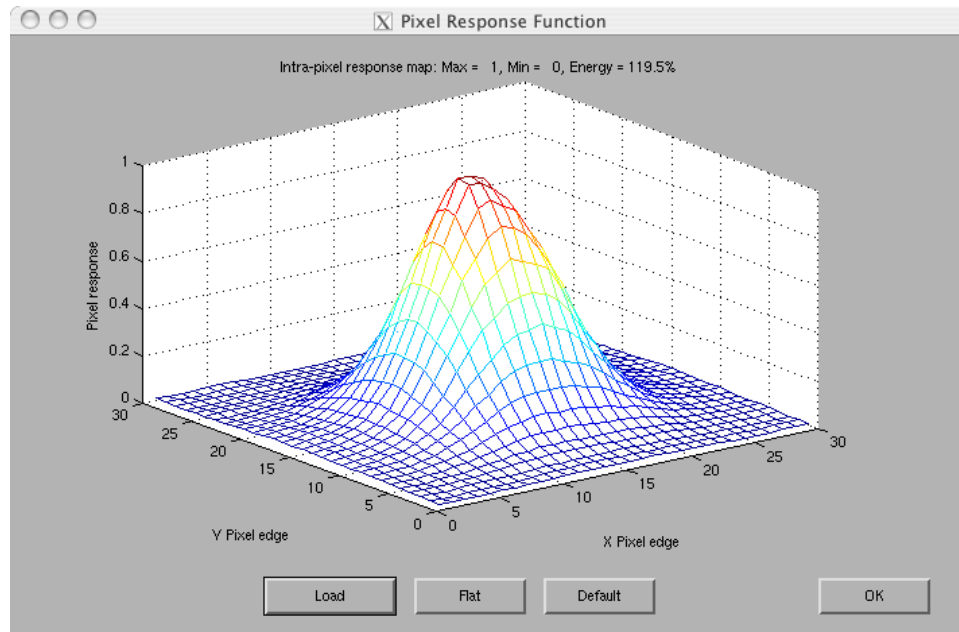
NEA variation with OTE focus and WFE



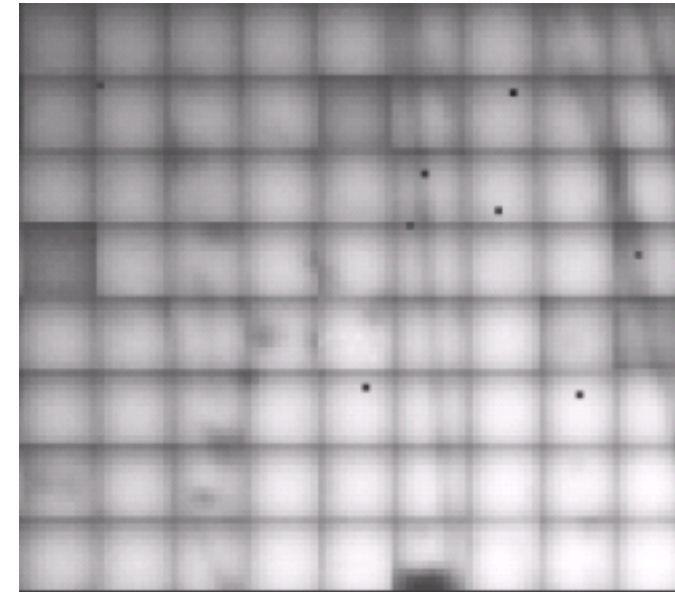
Top – models

Lower – measures from ETU





Model of pixel sensitivity for NEA calculation



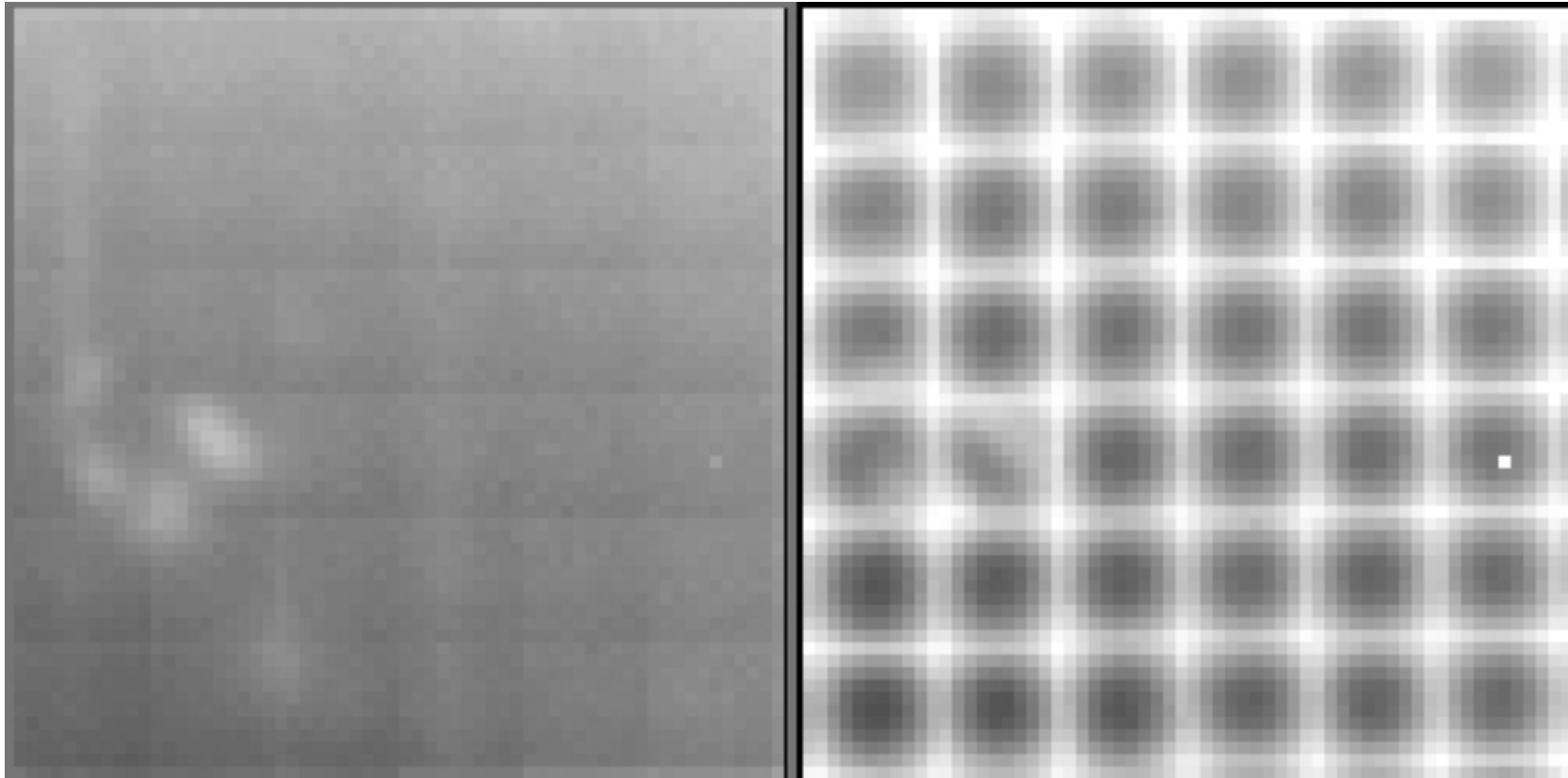
Map of intra-pixel variations



JWST detector intra-pixel sensitivity



HIA lab results at 2.2microns



Response corrected for charge spread

Raw response within pixels



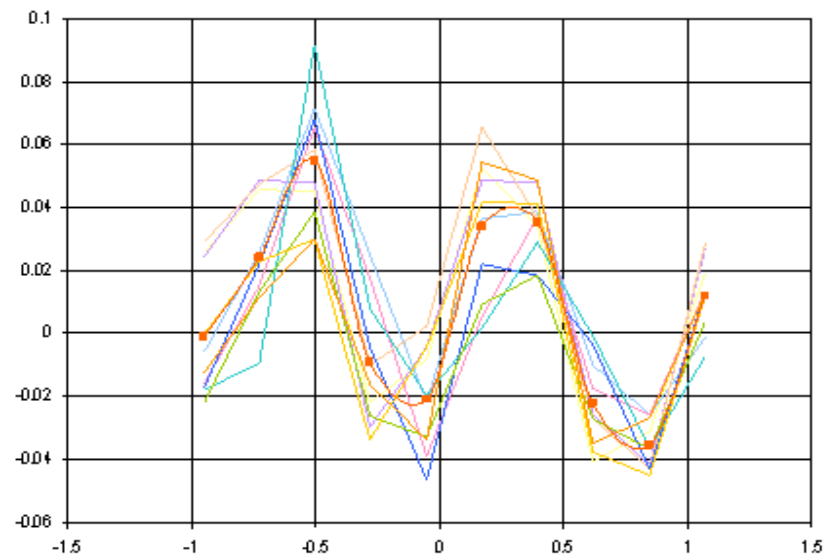
Guider: CNL measured from lab data

Systematic centroid offsets from pixel-sampled data



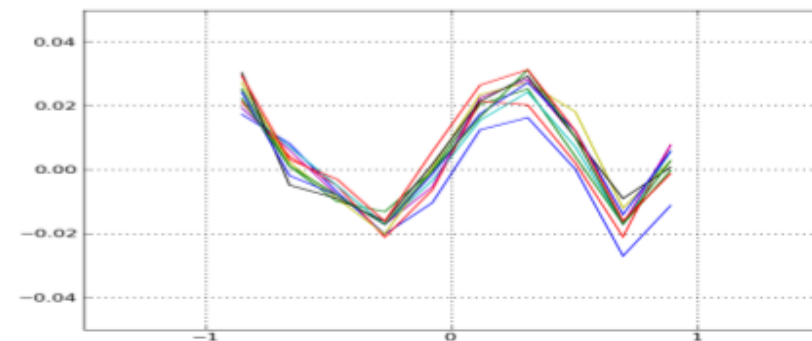
X-direction cuts through different places within detector pixel

This will be corrected for in reporting guider centroids



Signal 900e, 1.5 microns

2 mas

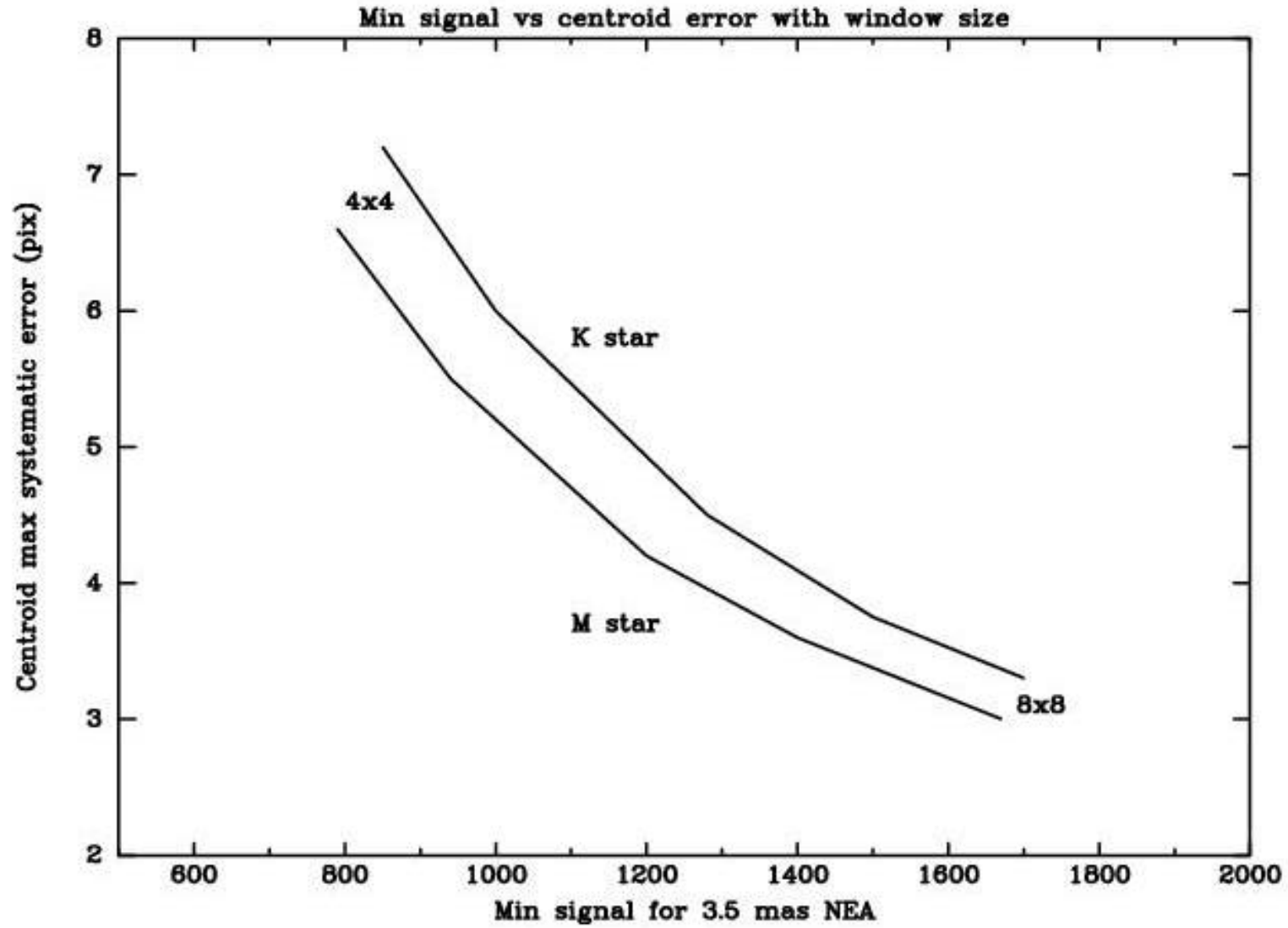


Signal 5000e, 3.2 microns

Verification of modelled performance, plus pixel-to-pixel non-uniformities, ongoing



Centroid offsets moving across pixels





Angular rates of Solar System objects seen by JWST



Object	Min. Rate (mas/sec)	Max Rate (mas/sec)	Distance Traveled in 10 hrs at Min Rate (asec)	Time to Travel 10 at Max Rate (hrs)
Mars	2.5	28.6	90.0	0.6
Jupiter	0.070	4.5	2.5	3.7
Jupiter, Io	0.004	10.2	0.14	1.6
Saturn	0.040	2.9	1.4	5.7
Uranus	0.020	1.4	0.7	17
Neptune	0.004	1.0	0.14	24
Pluto *	0.160	1.0	5.7	24
KBO	0.002	0.5	0.07	48

Adopted: linear tracking over FGS FOV at max 30mas/sec



Galactic coordinates of all known KBOs

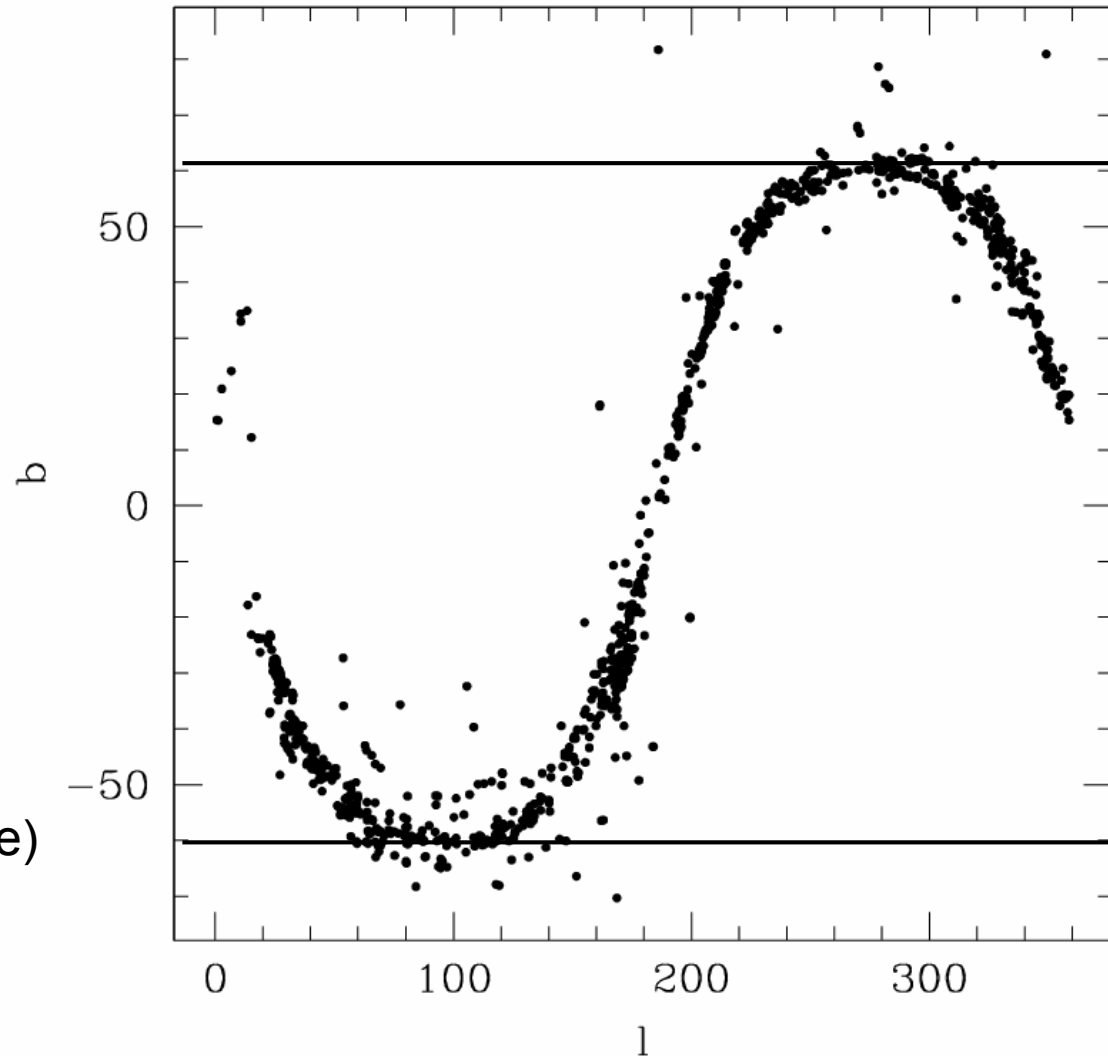


Compared with galactic poles:
At $b=60$ star counts up by $\times 1.6$
At $b=50$ star counts up by $\times 2.1$

From $J=19.4$ to 18.0 star
counts down by $\times 1.6$

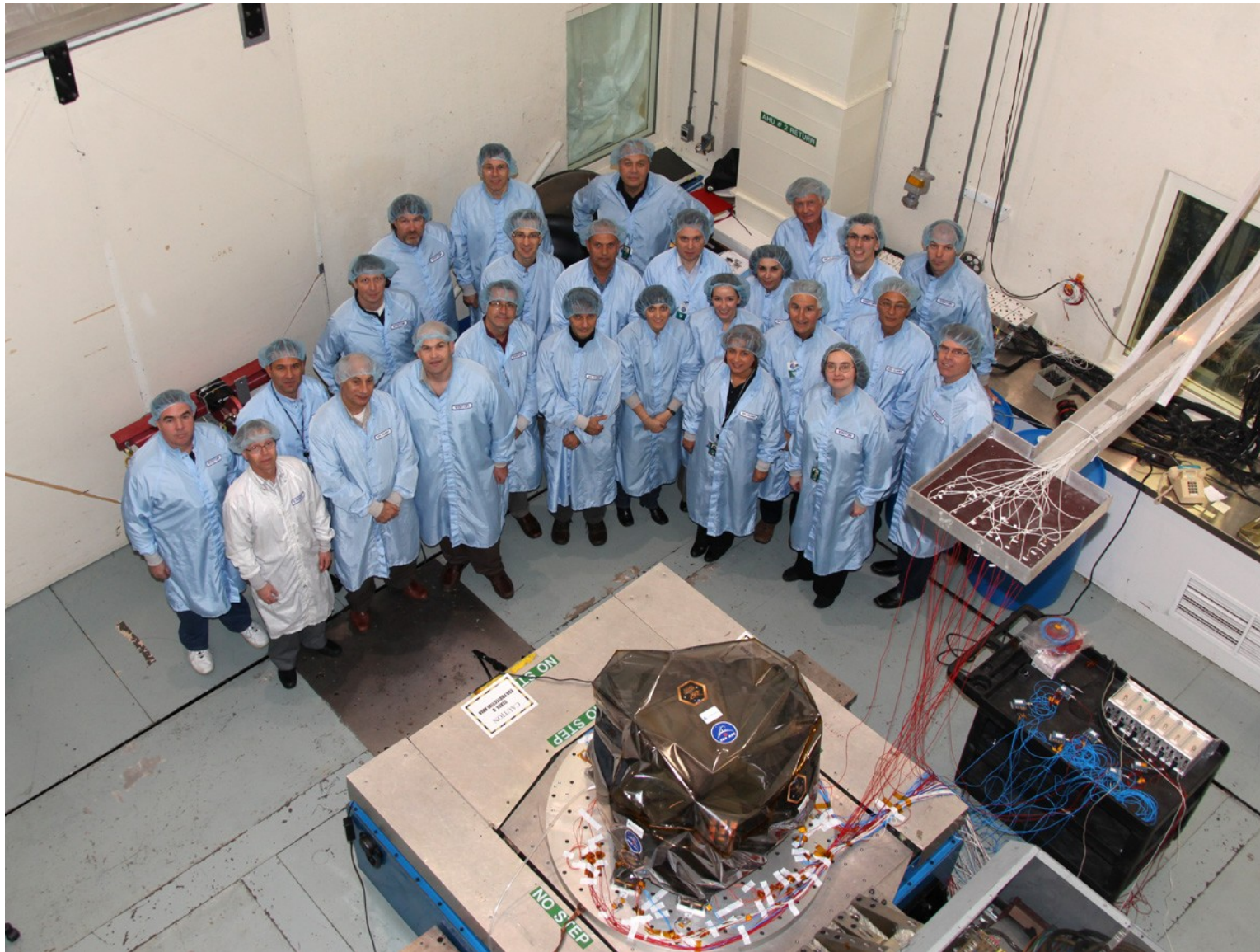
For almost all KBOs we have
>95% probability of GS giving
6mas in 32×32 guide box.

Extending the observing window
by \sim hours (FGS field crossing time)
will double the GS numbers again





ETU on DFL Vib table Oct 21

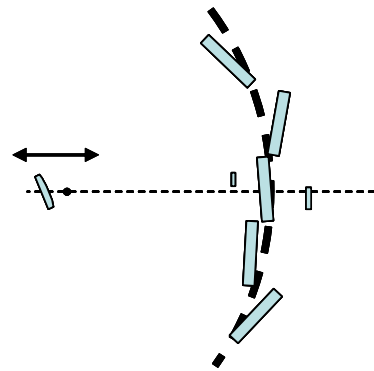




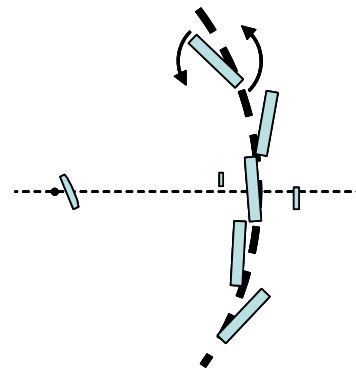
ID and acq issues



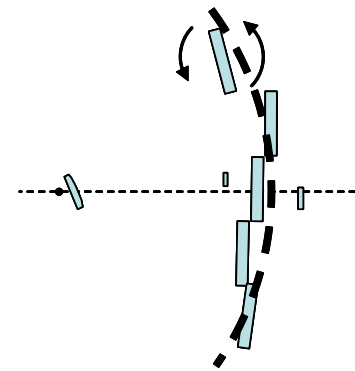
- Full field is read in strips to create ID map
 - Spacecraft is drifting, so strips should overlap to avoid losing stars
 - CRs are several times the GS faint limit signal
 - Double-reads needed to eliminate CRs
 - Pixel-to-pixel variations larger than star signals
 - Require CDS reads, and avoidance of first-frame settling
 - All this easily breaks original timing budget of 45 secs – up to 83 secs
 - Can reduce number of strips (i.e. FOV) and overlap to save time
 - Tradeoff between time and success rate
-
- There are several non-GSC stars and compact galaxies per FOV
 - Can guide on close doubles and compact galaxies, unlike HST
 - All above affect the ID success rate and/or observing efficiency
 - Plan Monte-Carlo runs for ID success stats by FGS team at STScI



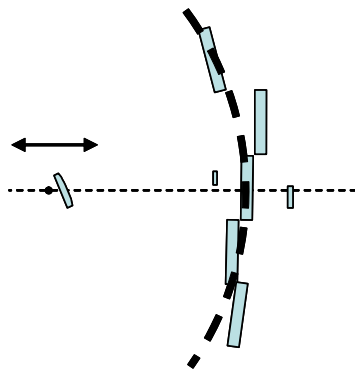
First Light: Focus Sweep of SM



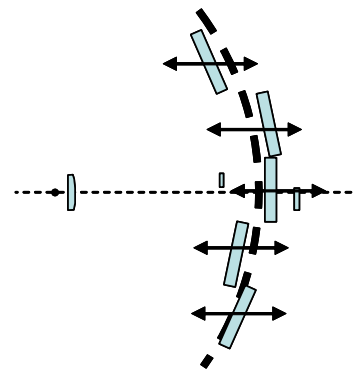
First Light: Segment Identification



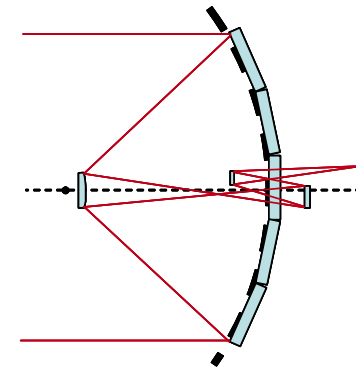
First Light: Image Placement



Global Alignment: Focus Sweep of SM



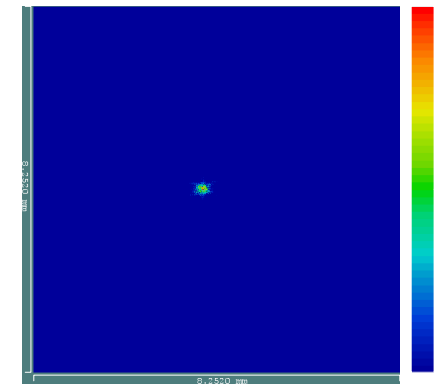
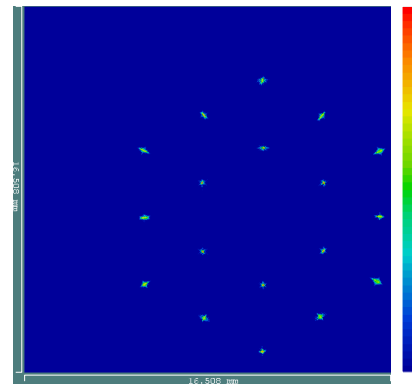
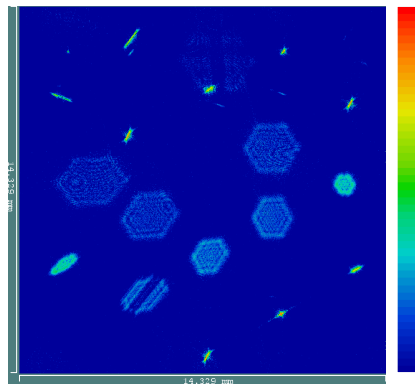
Coarse Phasing: Adjustment of Segment Pistons



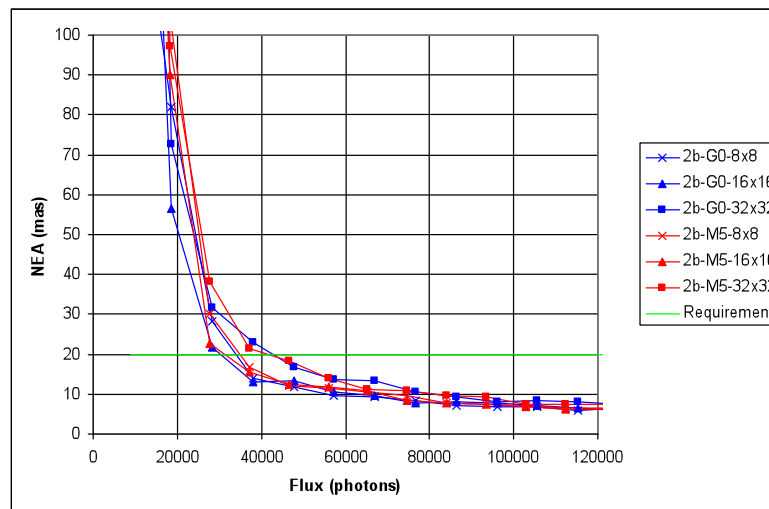
Fine Phasing: Fine Tune all OTE Degrees of Freedom

- WFSC must capture and correct the initial post launch state of the OTE,
- It must sense the WFE of the Secondary and PMSA to 10 nm of WFE each
- It must unambiguously correct the Low Spatial Frequency WFEs of the OTE to within 19 nm over the FOV of the OTE

Steps in primary phasing



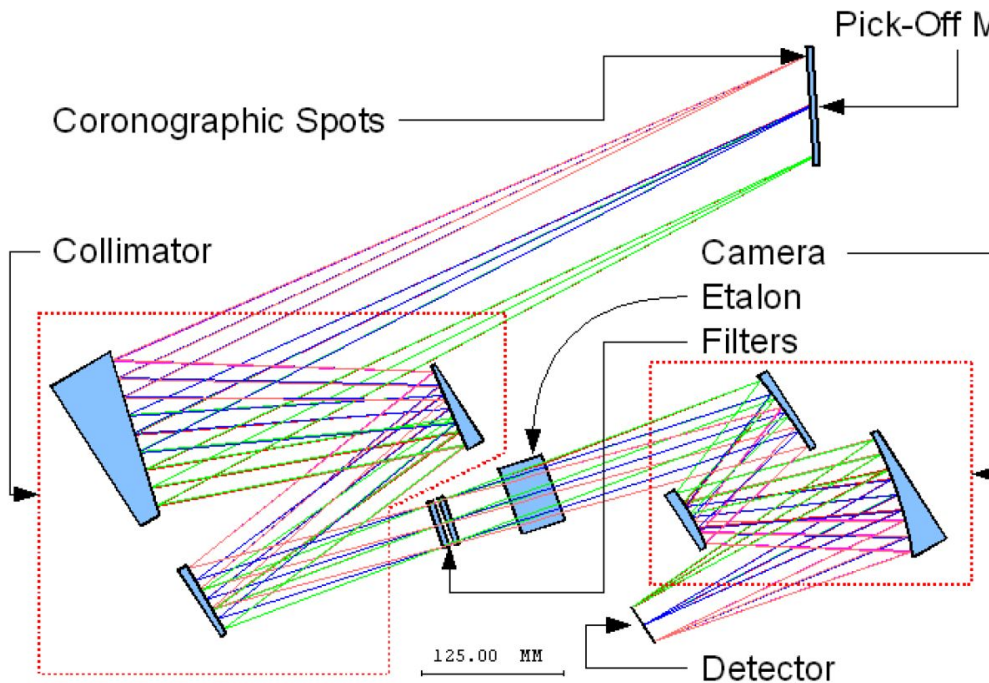
Guiding performance modelled for all cases.



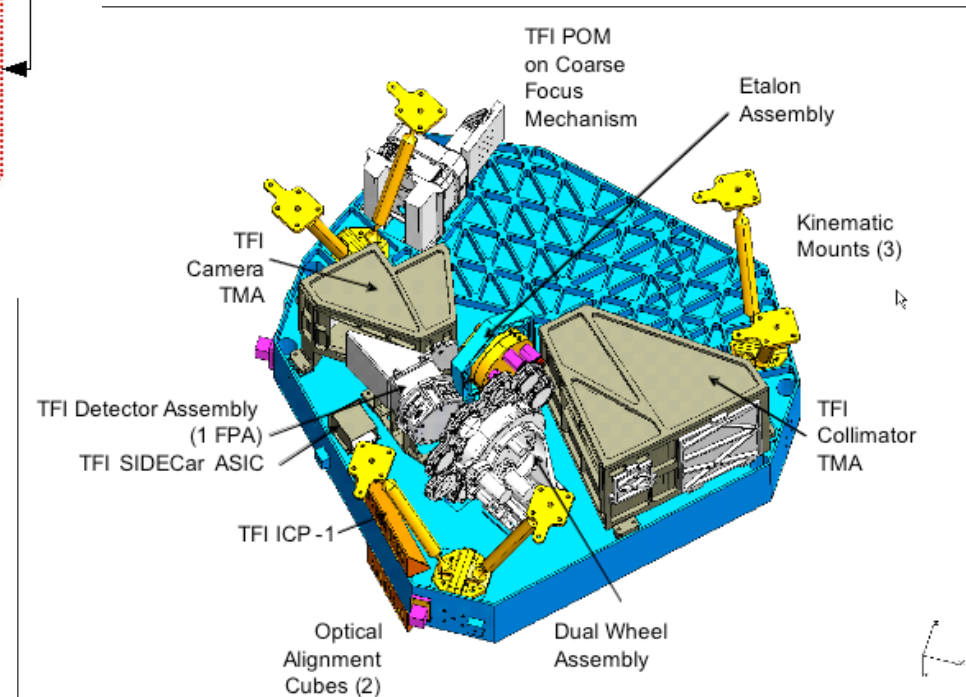
Little difference between G0 and M5 guide star types.

Require isolated star of mag ~14.5

TFI design



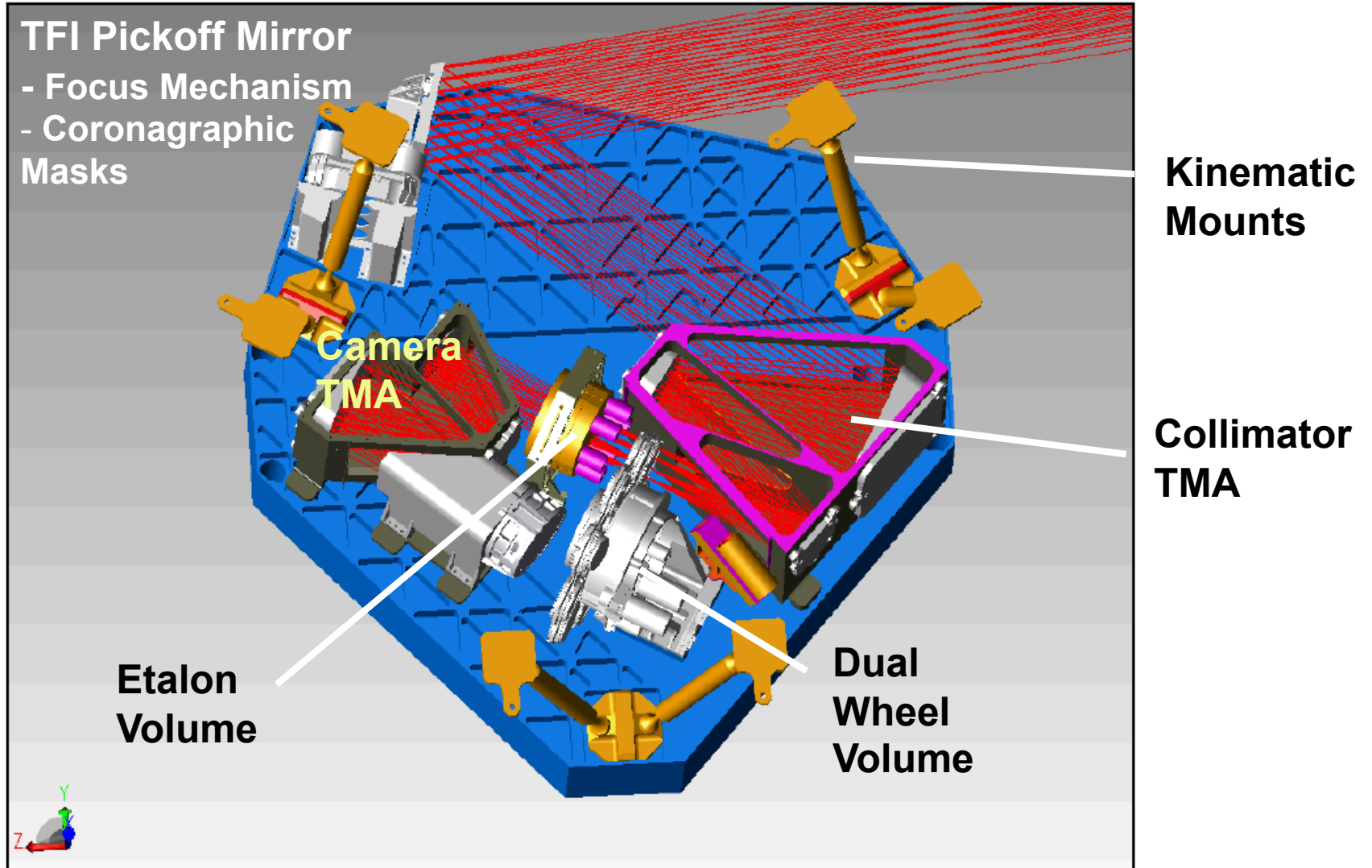
- All reflective optics, except etalon & blocking filters
 - 79 nm rms wave front error
- Dual wheel for blocking filters and masks



Optical Subsystem – TFI Layout



Light from JWST Telescope



TFI Optical Assembly



TFI at a glance

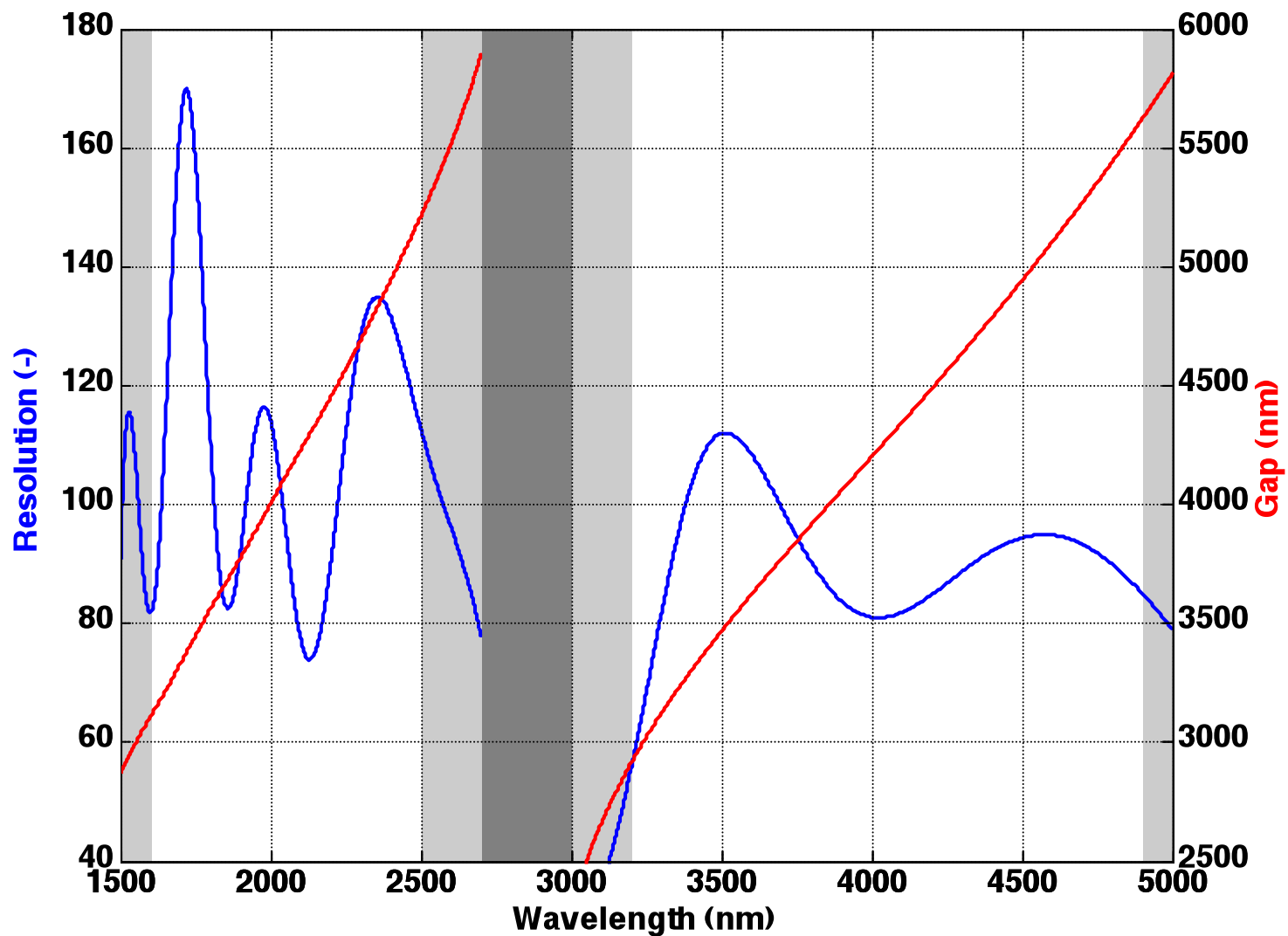
- FOV: 2.2'x2.2'
 - 65 mas pixel sampling (Nyquist at 4.0 μm)
 - 2048x2048 pixels (Hawaii 2RG)
- Wavelength range: 1.6-2.6 and 3.2-4.9 μm
 - (actually 1.5-2.7 μm and 3.1-5.0 μm)
- Resolving power of ~ 100 (80-120)
- Sensitivity, 10σ 10x1000 s
- Operating modes
 - Normal imaging
 - Lyot coronagraphy
 - 4 occulting spots, 3 lyot masks
 - Non-Redundant Masking interferometry (NRM)



Wavelength μm	Sensitivity nJy	Sensitivity mag
1.5	149	24.8
2.0	139	24.3
2.5	119	24.1
3.5	110	23.5
4.0	136	23.1
4.5	142	22.8



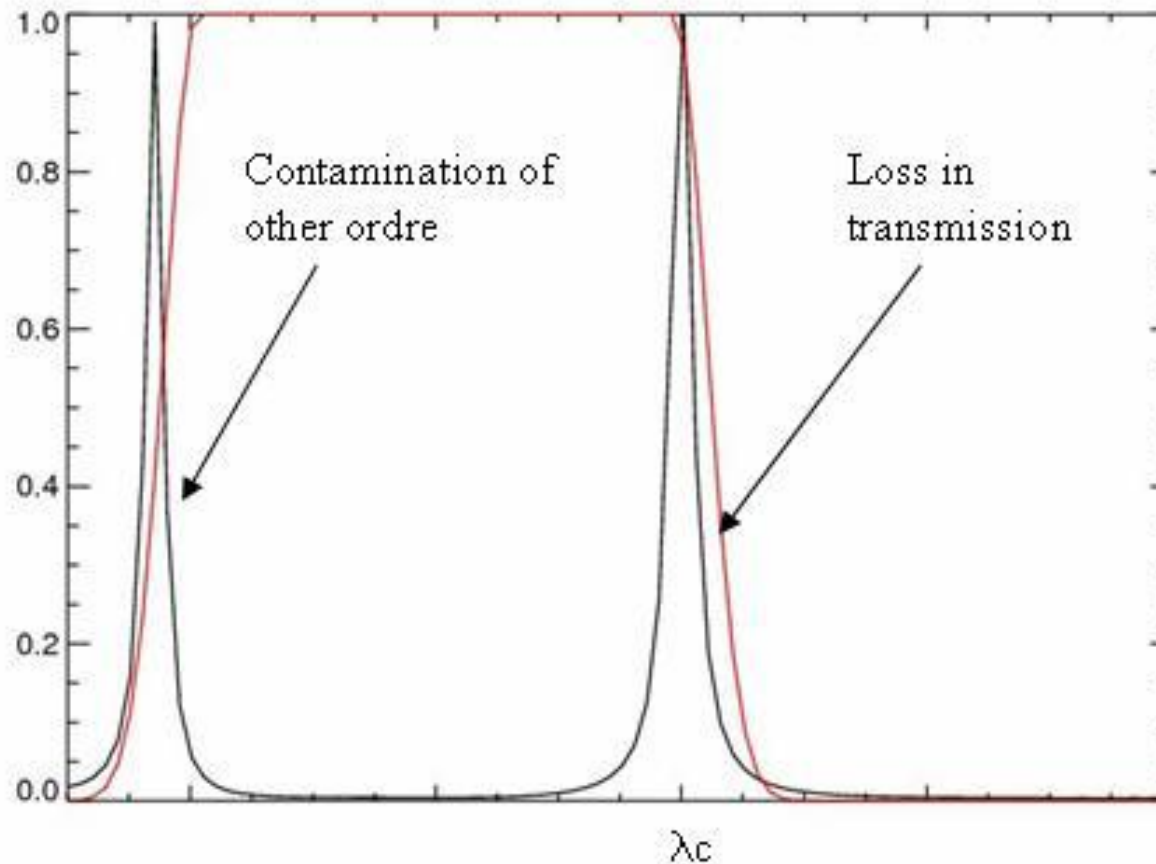
Spectral Resolution



Filter is defined ($\lambda_c, \Delta\lambda$) so that ...

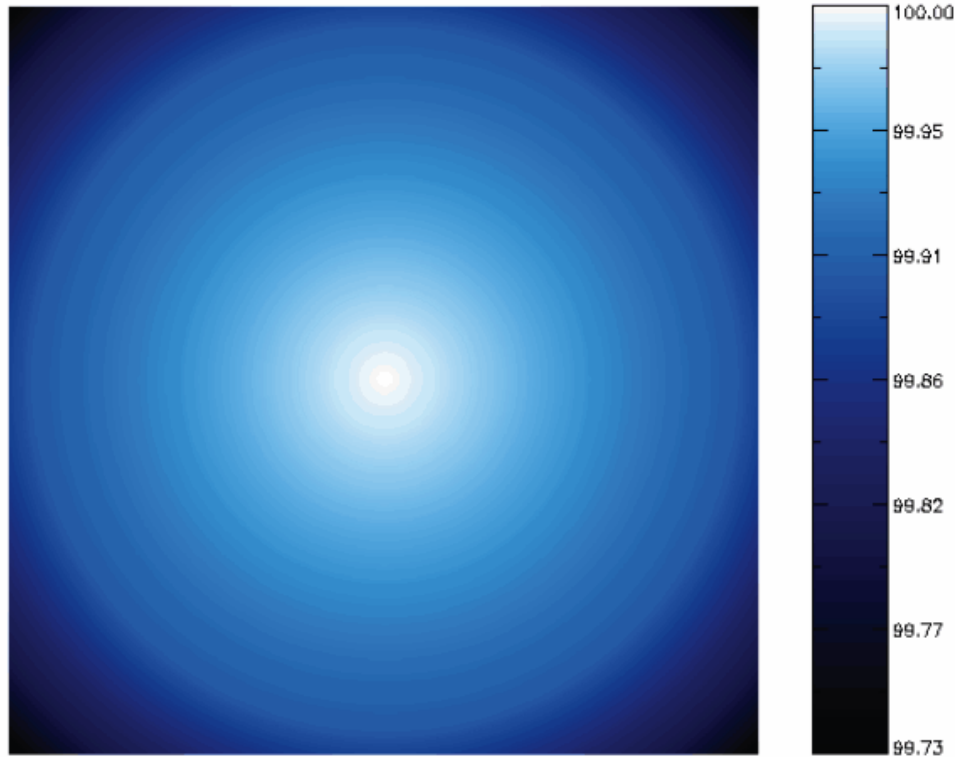


- Transmission is maximized over the working interval
- Contamination from other orders is minimized



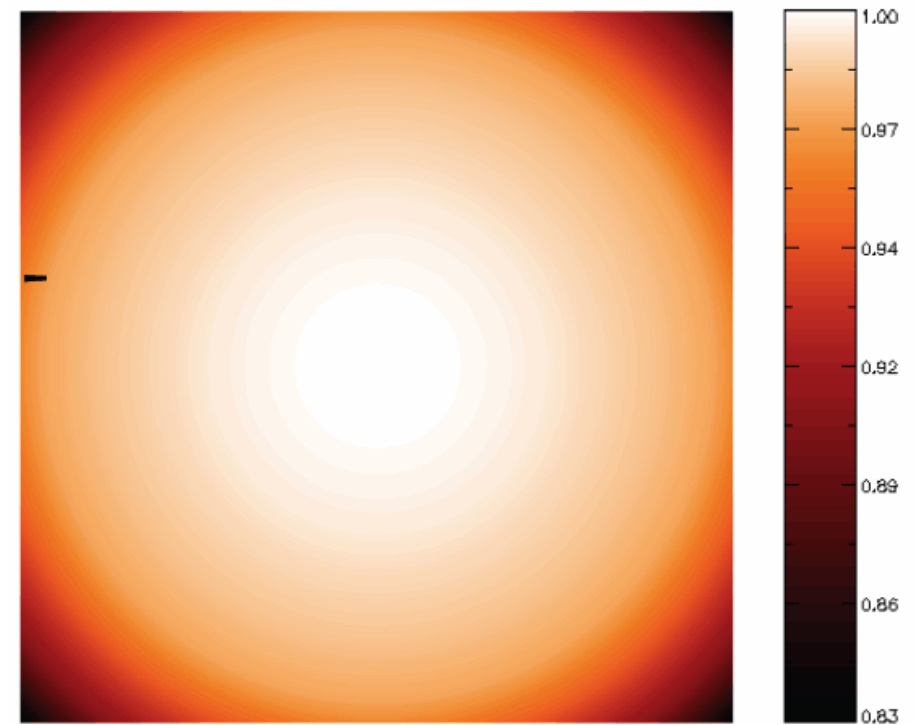
Spectral/spatial uniformity

~0.1% wavelength shift at edge of field



Blue shift (% of λ) - $2\mu\text{m}$

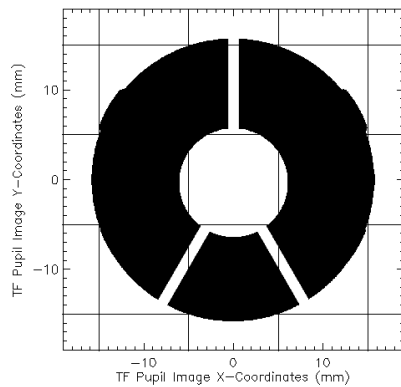
~4% drop in flux at edge of field for perfectly monochromatic source



Transmission - $2\mu\text{m}$

Coronagraphy (Lyot coronagraph)

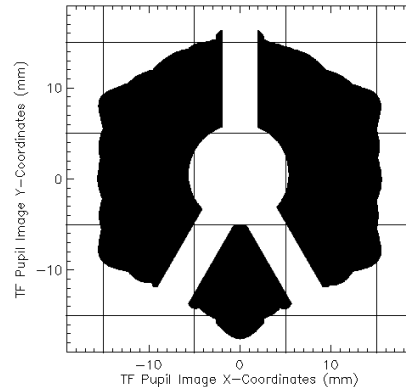
- 4 occulting spots engraved on pick-off mirror
 - Diameters of 0.58", 0.75", 1.5" and 2.0"
- 3 lyot masks
 - Transmissions of 71%, 66% and 21%
 - Robust against pupil shear of up to 4%



C71

0.58" and 0.75"

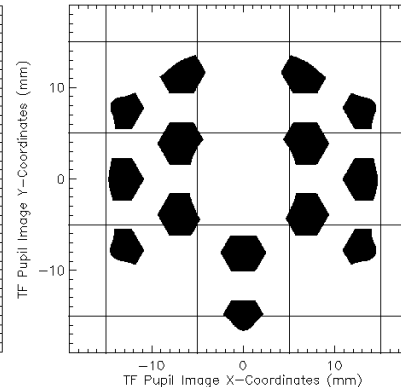
<1"



C66

1.5"

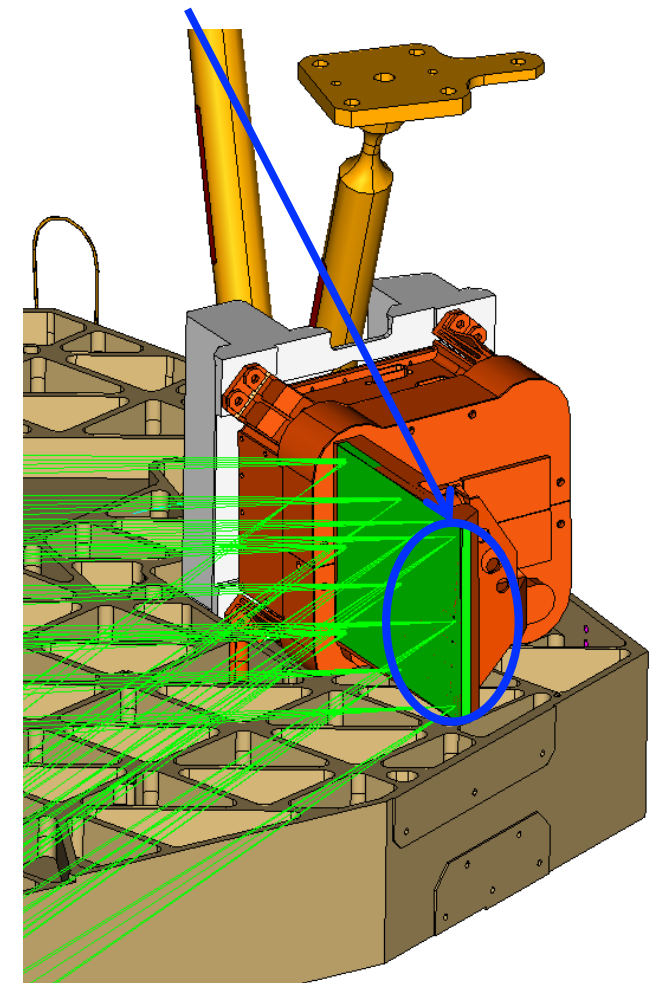
1"-2"



C21

1.5" and 2.0"

>2"

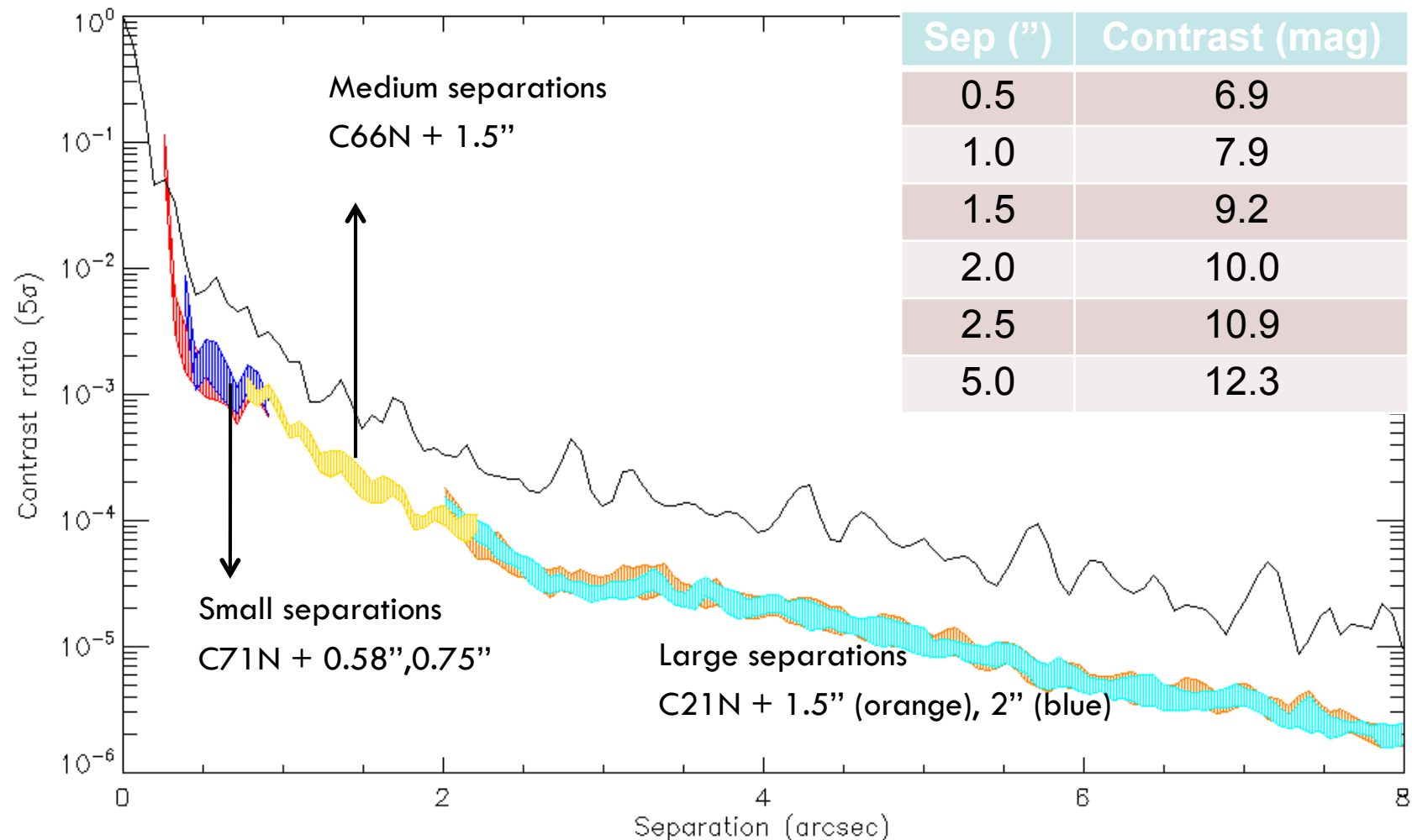




Coronagraphy contrast limits (3% pupil shear)

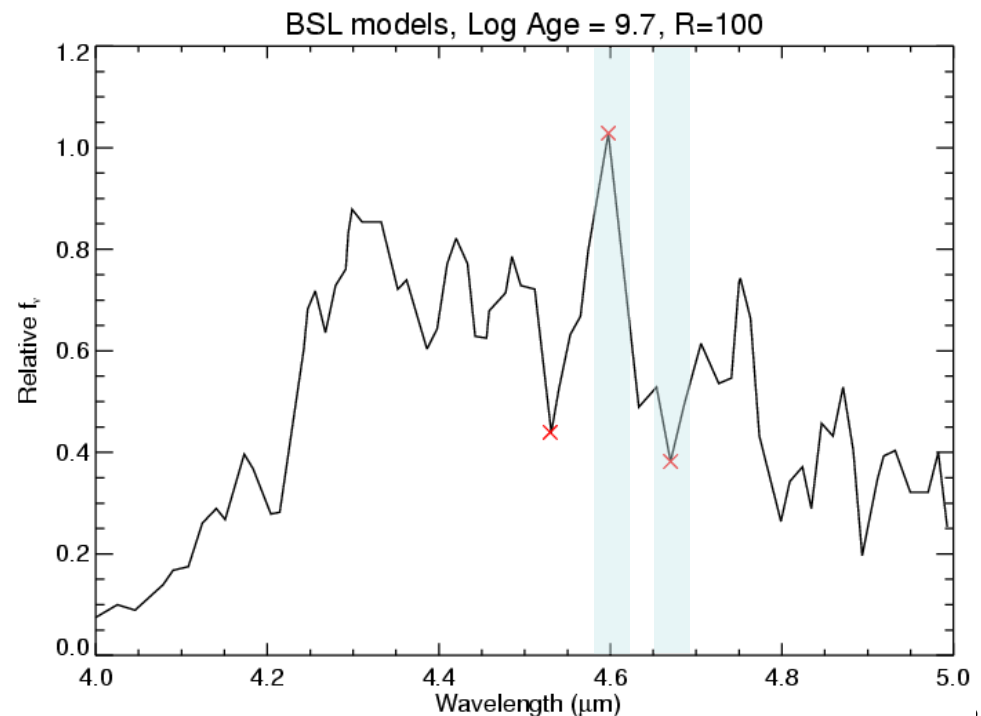


These contrasts can be improved further with PSF subtraction



Differential imaging with TFI

- Reference star PSF subtraction
 - Narrow-band relieves requirement of similar spectral shape within band (speckles are chromatic)
 - May perform better than for other instruments
- SDI (Spectral Differential Imaging)
 - Unique to TFI
 - Can be used in addition to reference star PSF subtraction
 - Simpler than roll subtraction (which other instruments may require)
 - There are several spectral features suitable for SDI in exoplanet spectra

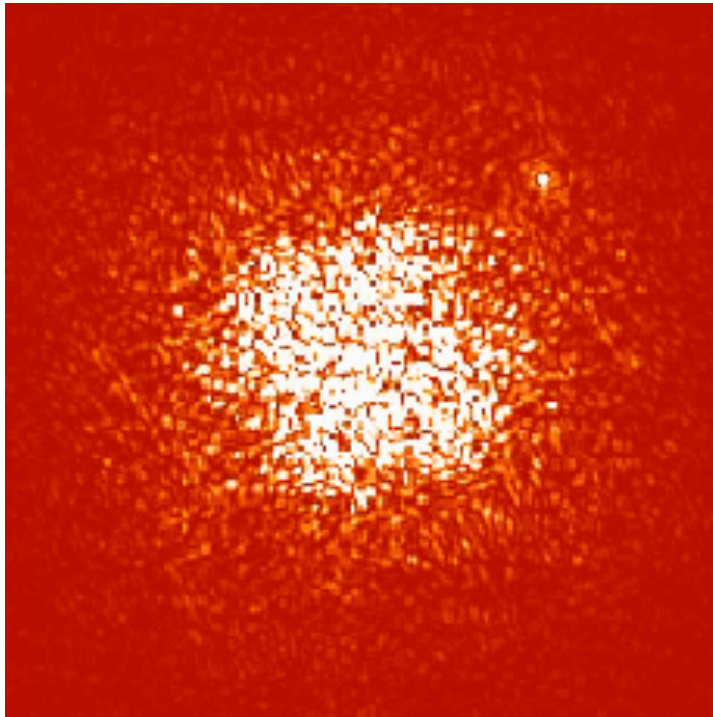


Case for 4-5 μm λ coverage: Exoplanet SEDs

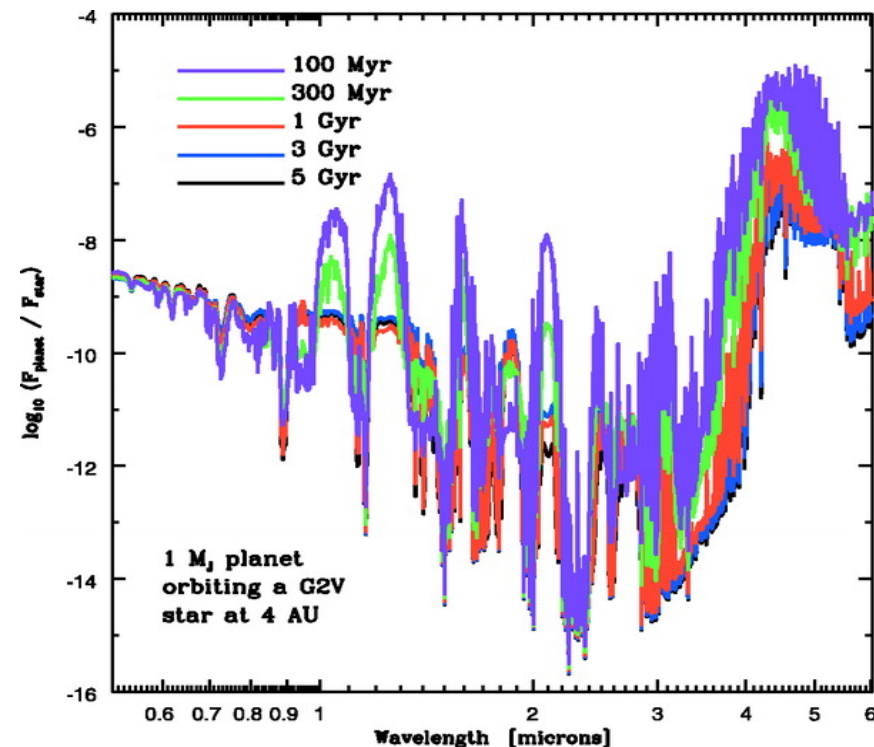


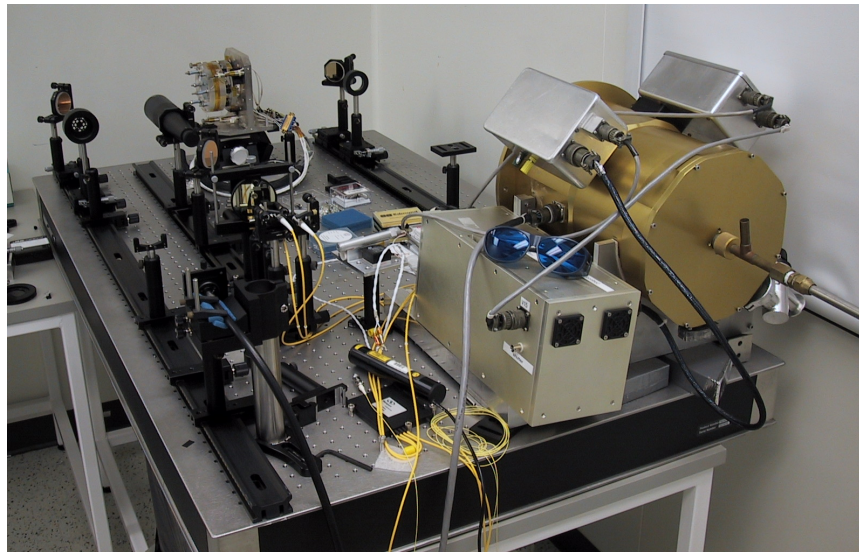
- Identification and statistics of extrasolar planets: direct observation
- Scan through wavelengths of maximum planet/star contrast
- **The combination of coronagraphy and TFI wavelength scanning is ten times more sensitive than other JWST fixed filter observations.**

TFI planet detection simulation:
Monochromatic PSF movie: 4 to 5 μm

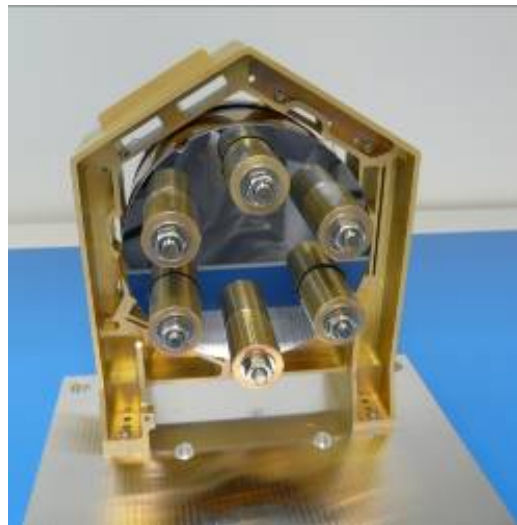
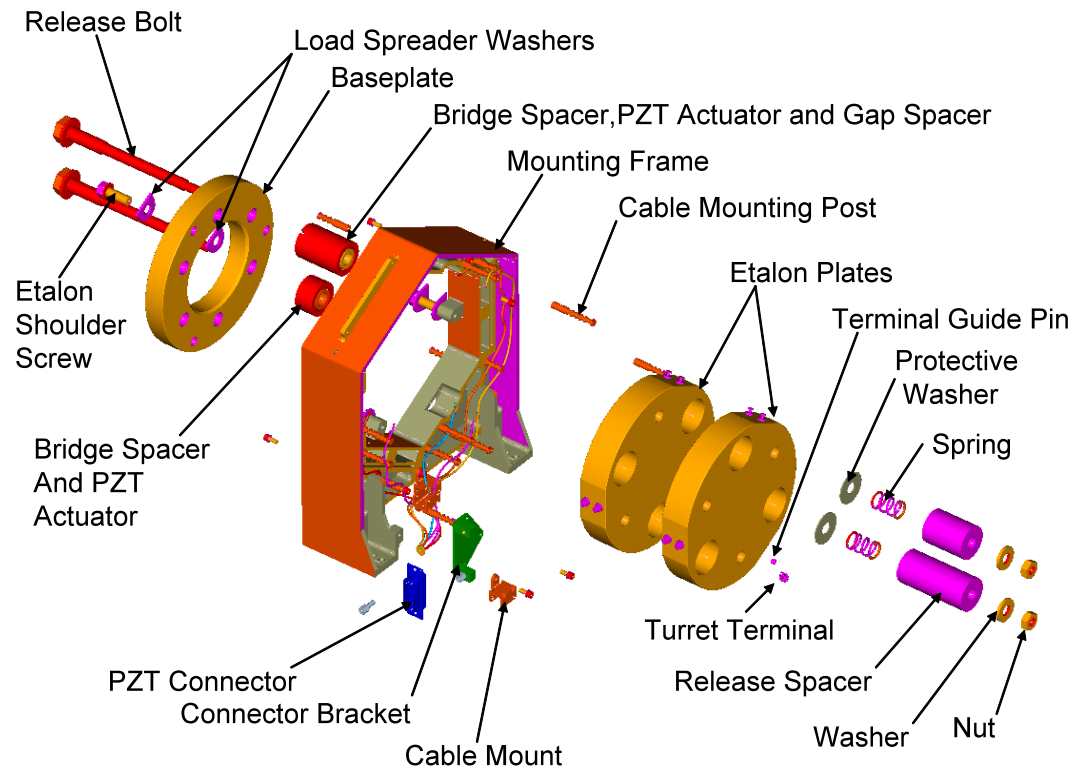


Planets are bright at 4-5 μm



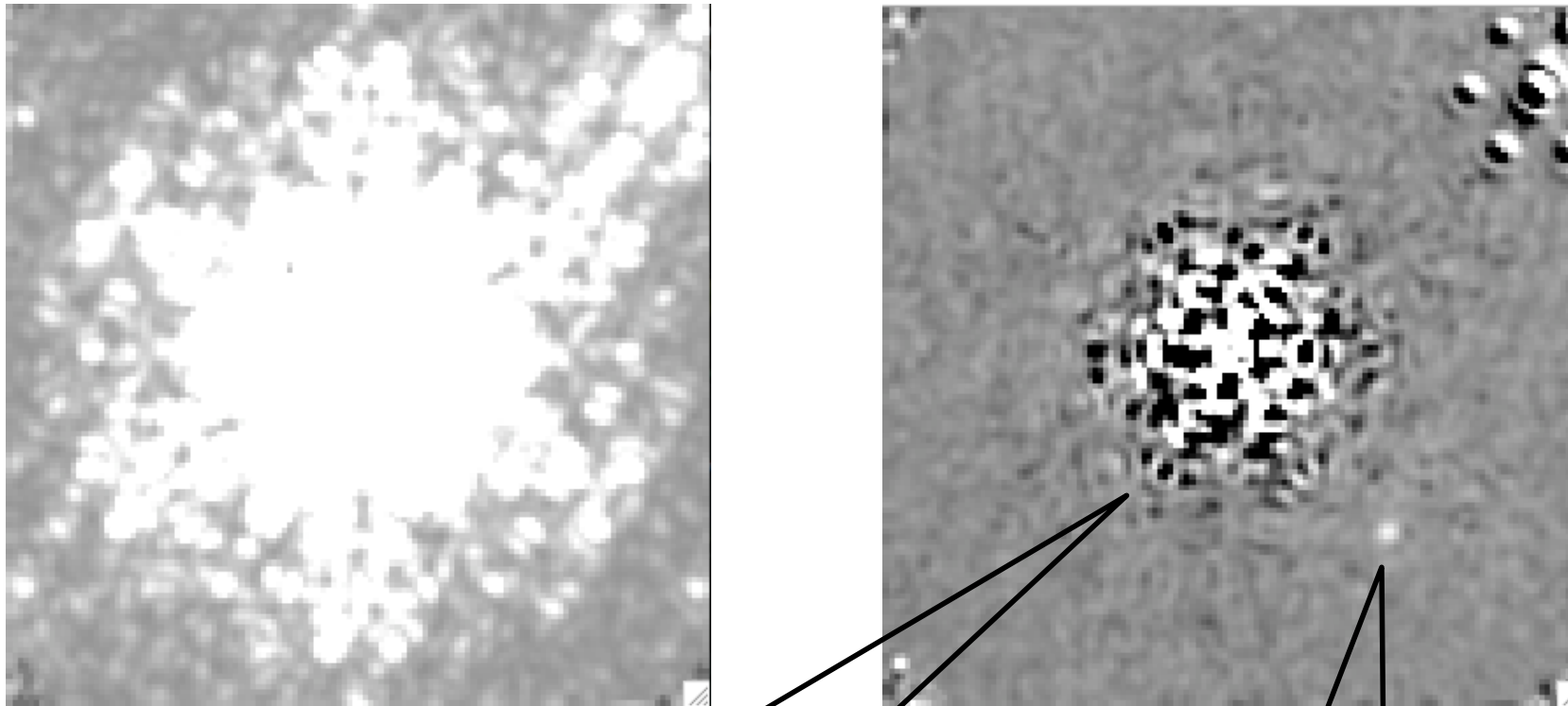


U de Montreal lab model



Flight design test

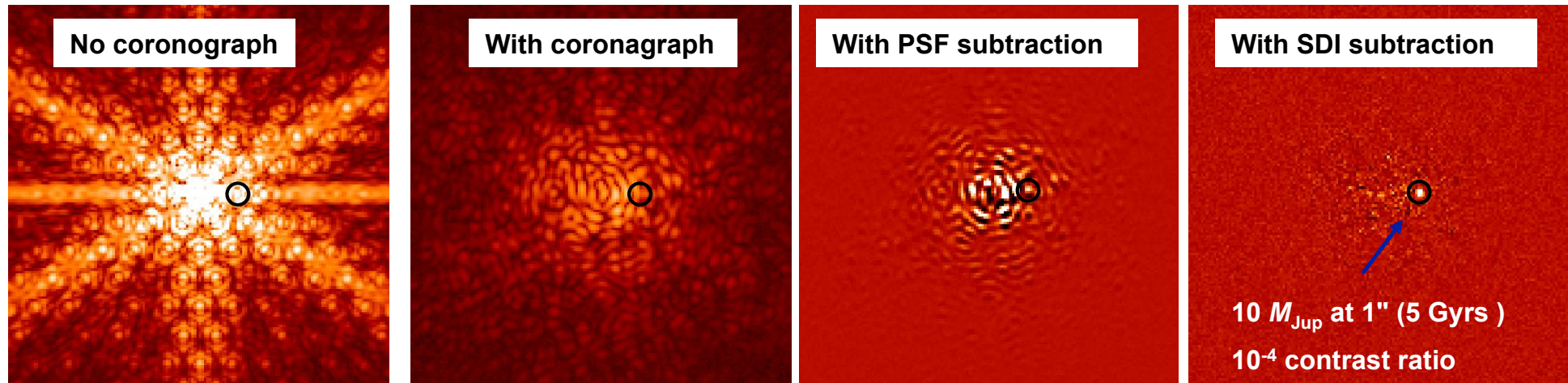
U de Montreal lab results



Subtraction from two
adjacent wavelengths

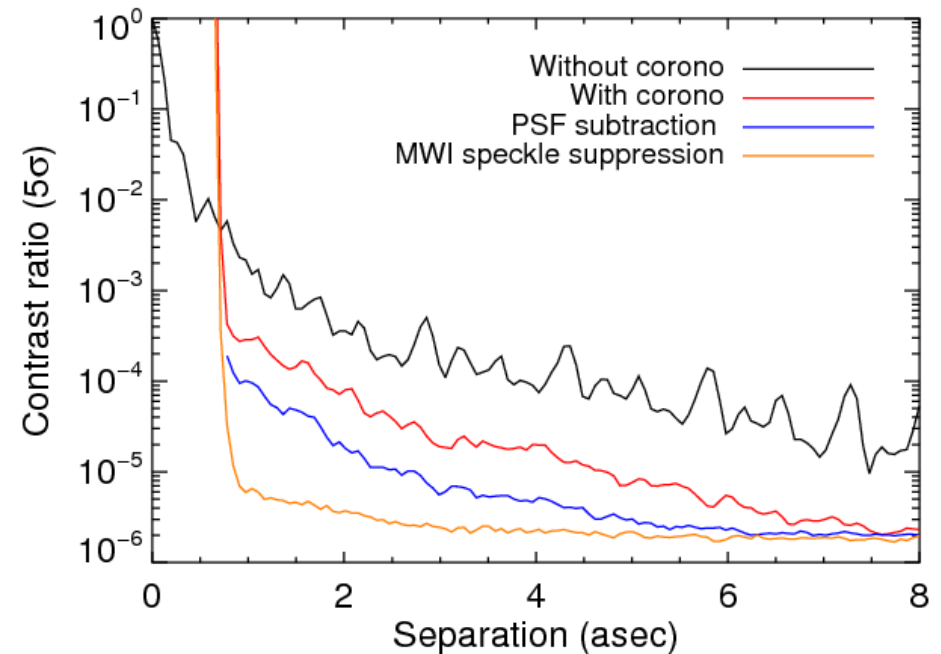
Companion
10000
fainter

Summary: TFI can achieve excellent contrast



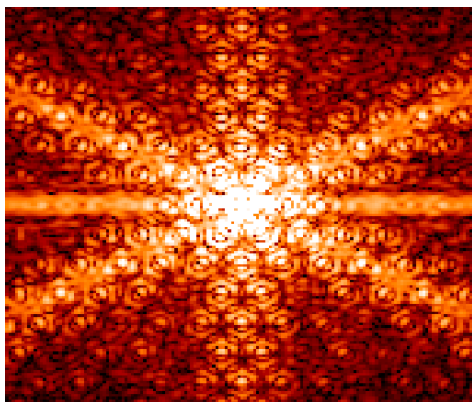
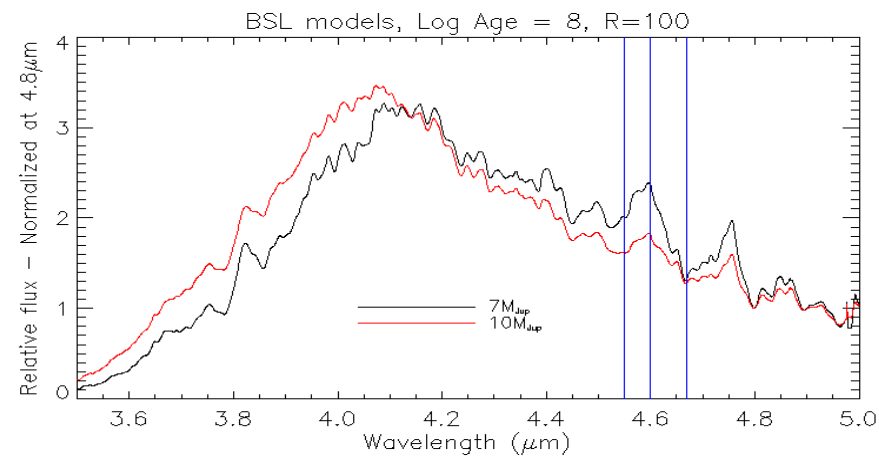
- Contrast of $\sim 10^{-5}$ possible at $>1''$

Simulation: M. Beaulieu

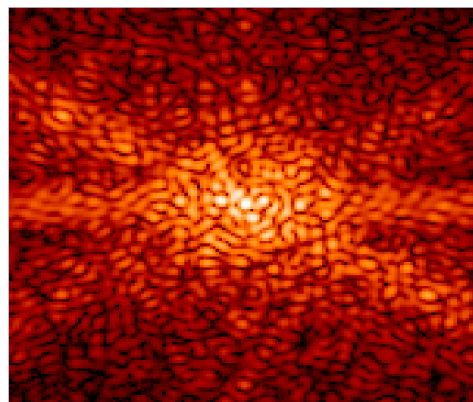


HR 8799 seen with TFI

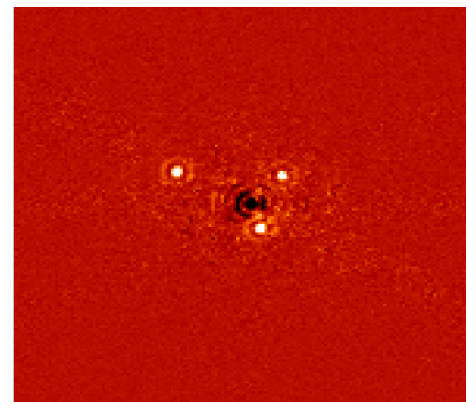
- Example shown with SDI
 - 3λ
- Could use reference star PSF subtraction instead



Without coronagraph



With coronagraph



With SDI

Simulation:
M. Beaulieu



Non-Redundant Masking interferometry

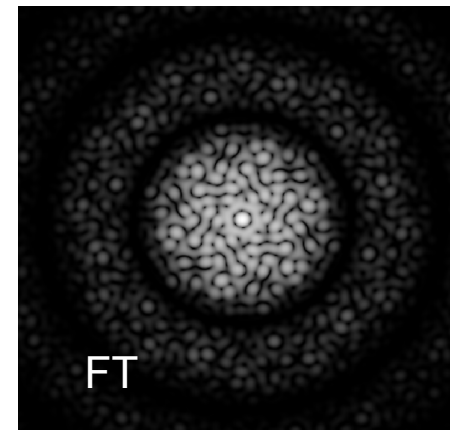
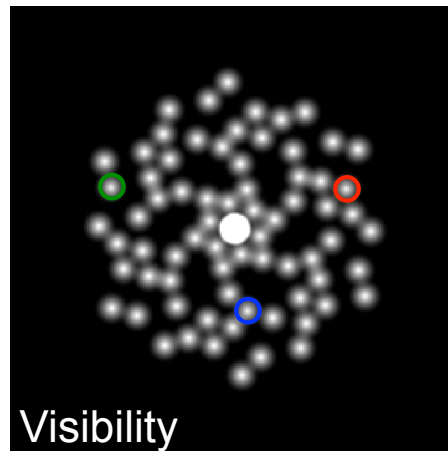
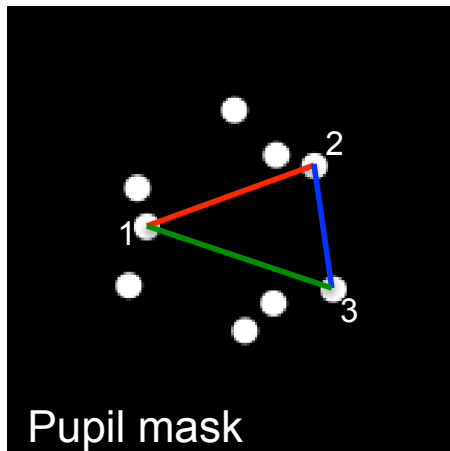


Mask containing multiple small apertures at a pupil plane

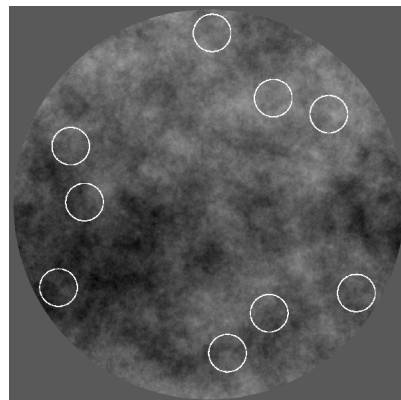
No line joining any two sub-aperture has the same length and PA as another one
From FT of interferogram, amplitude & phase of interference fringe coming from each pair can be measured

Fit a model to measured phases and amplitudes

- **Better resolution** Two sources can be resolved for a separation of $0.5 \lambda/D$
- **Better contrast at small separations** Wave front phase errors have little effect on closure phase

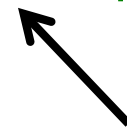


Phase error



Measured = true + phase error + meas. error

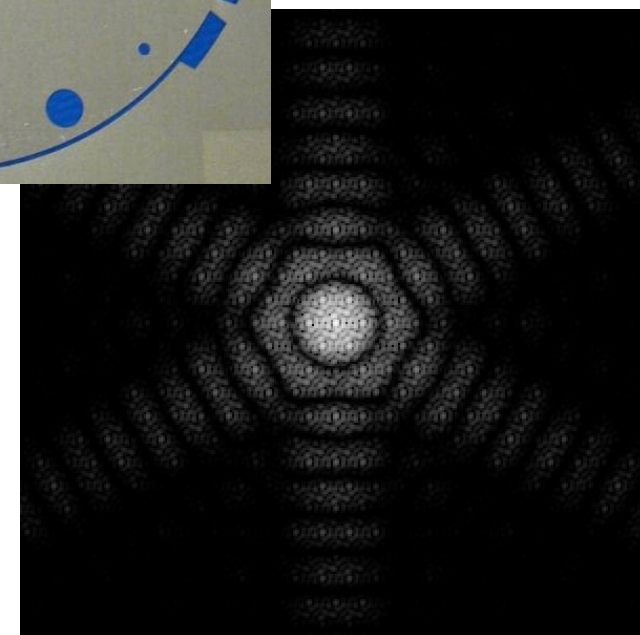
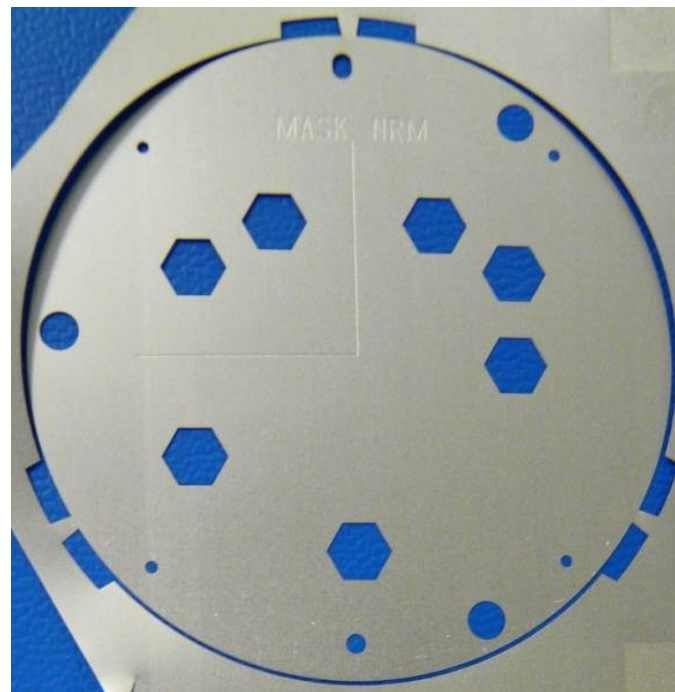
$$\begin{aligned} \phi(2-1) &= \phi_0(2-1) + \psi_2 - \psi_1 + \epsilon_{12} \\ \phi(1-3) &= \phi_0(1-3) + \psi_1 - \psi_3 + \epsilon_{13} \\ \phi(3-2) &= \phi_0(3-2) + \psi_3 - \psi_2 + \epsilon_{32} \end{aligned}$$



Sum these (closure phase) and phase errors cancel out

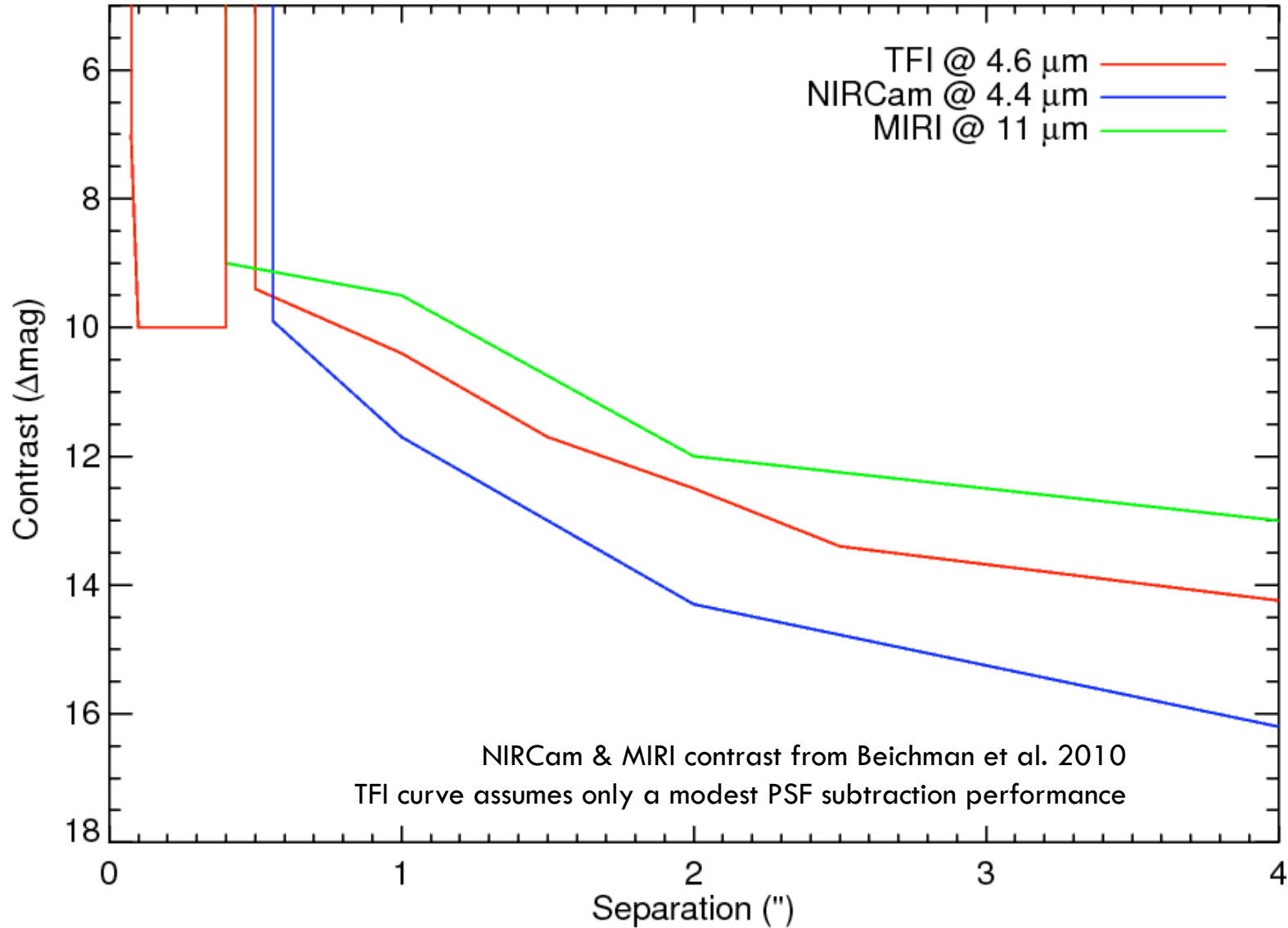
TFI Non-Redundant Mask

- 7 apertures
 - 5.28 m longest baseline
 - 1.32 m shortest baseline
- Throughput
 - 15%
- Resolution ($\lambda/2B_L$)
 - **≈ 75 mas at $4.6 \mu\text{m}$**
- Nominal FOV ($\lambda/2B_S$)
 - **$\approx 0.4''$ at $4.6 \mu\text{m}$**
- Contrast sensitivity
 - **≈ 10 mag**





TFI/NRM defines unique capability

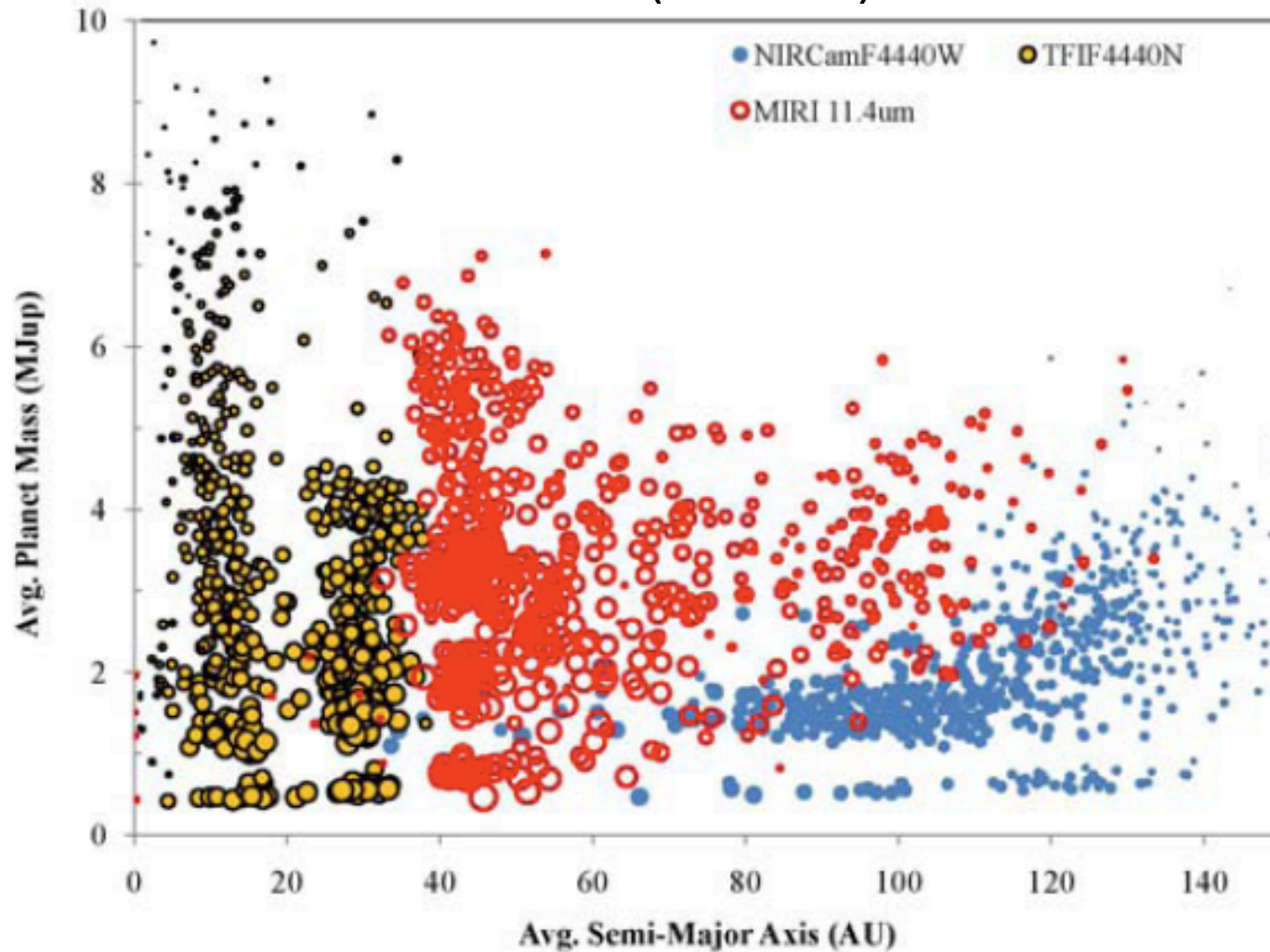




TFI/NRM will be a powerful tool for finding young planets within 30 AU

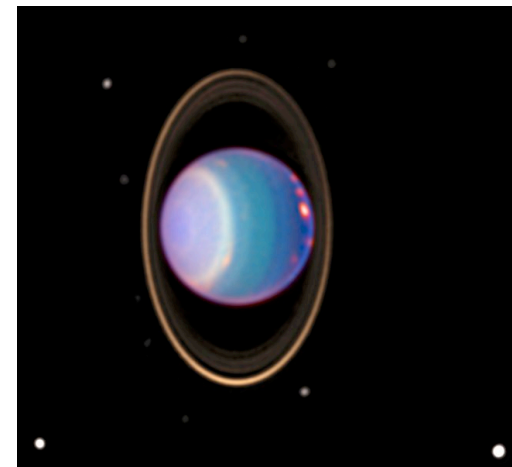
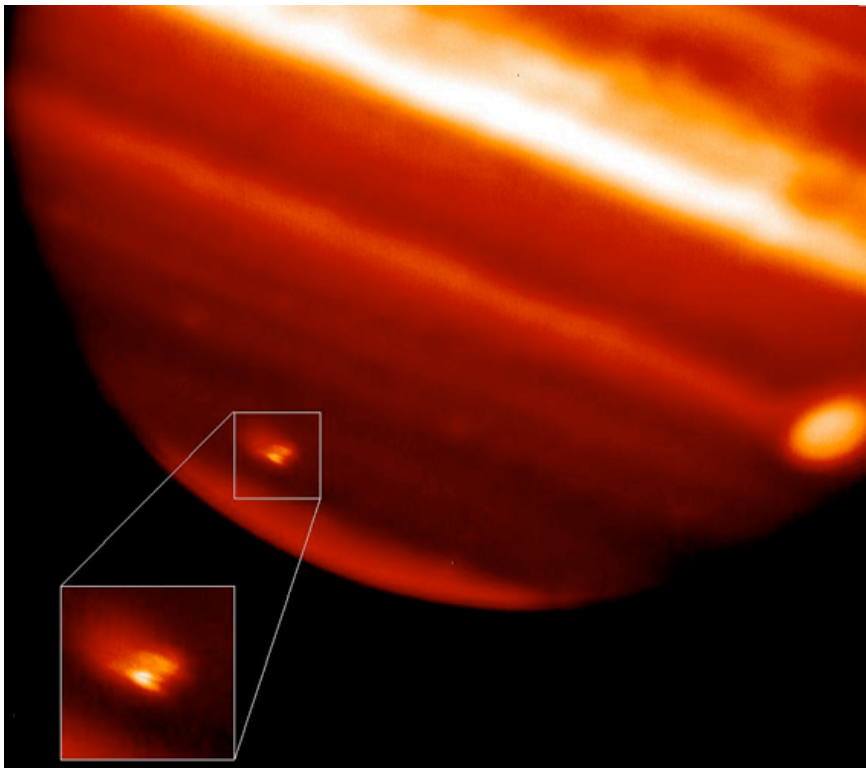


Beichman et al. (submitted)



A note on solar system planets

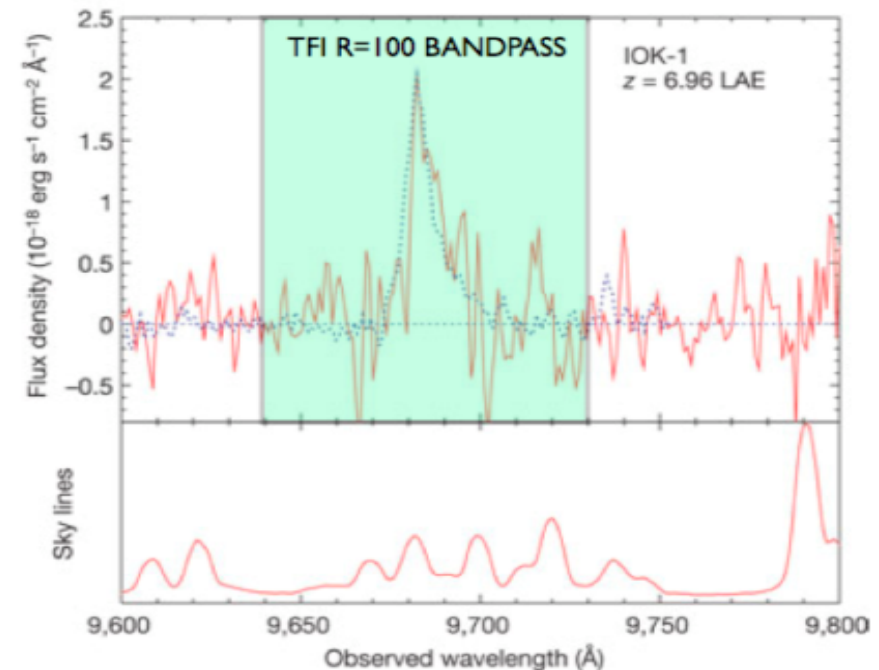
- TFI could be the only instrument on JWST for (spectral) imaging without saturation – rapid subwindow read and narrow bandpass



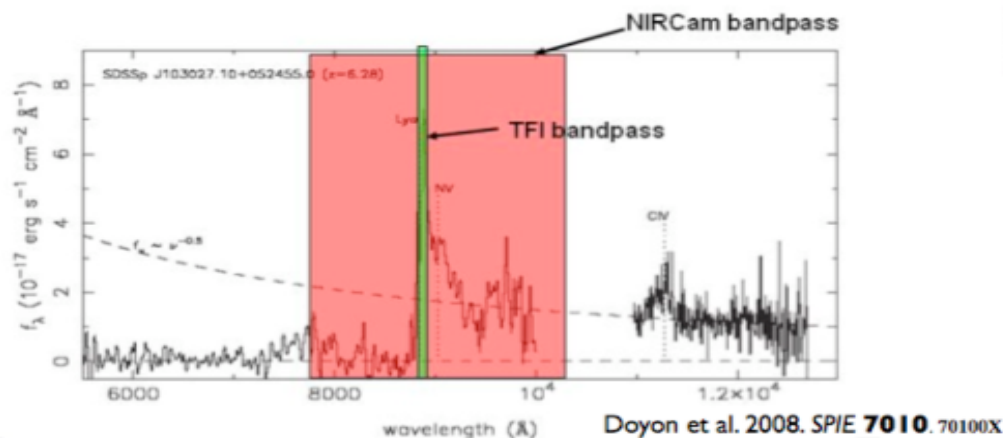
High-Redshift Science with TFI

- * TFI wins by detecting line emission in faint objects.
- * Lyman Alpha Emision can be up to 20x as bright than the continuum for a Lyman Alpha Emitting (LAE) galaxy.
- * $L\alpha$ is redshifted into the TFI λ range for $z \sim 10-30$, covering the era from the dark ages to *first light* where the universe becomes reionized

LAE galaxy at $z=6.96$



Iye et al. (2006). *Nature* **443**. 186



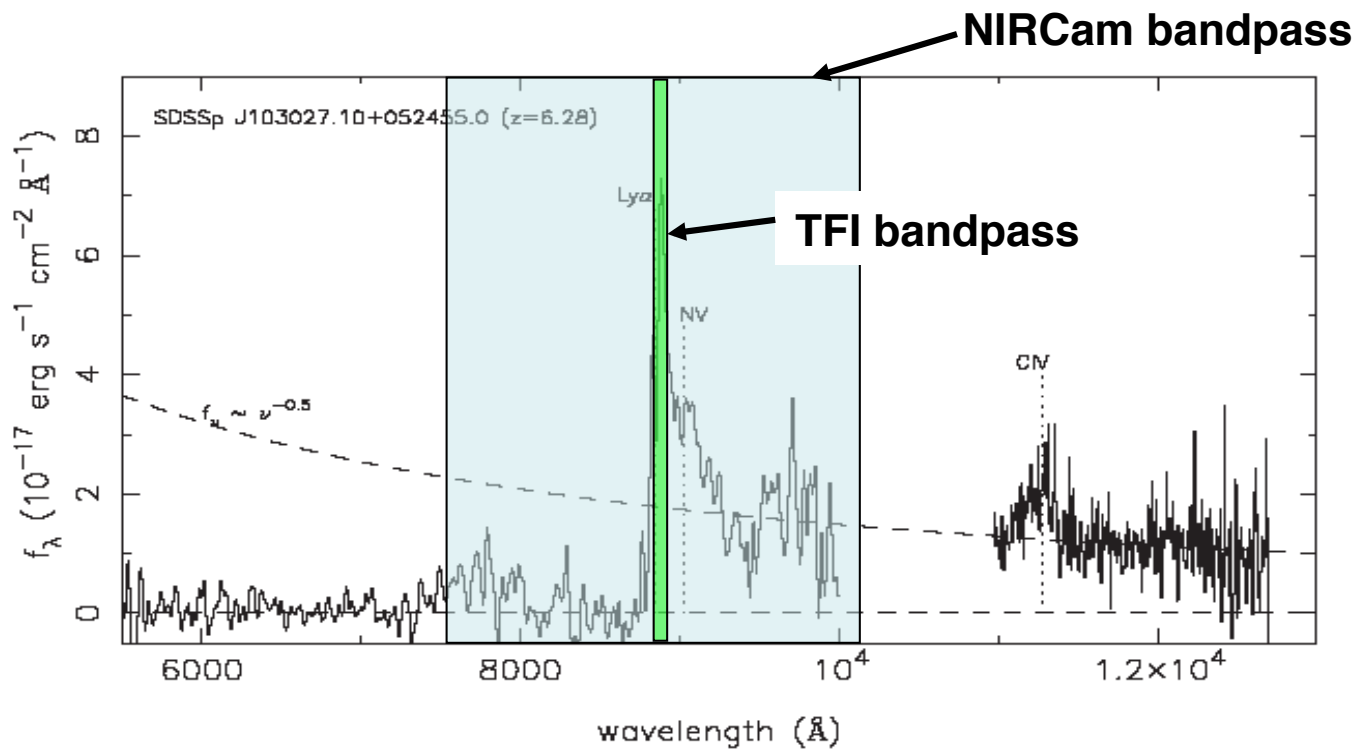
Doyon et al. 2008. *SPIE* **7010**. 70100X

- * Its relatively small bandpass yields higher S/N than NIRCam broadband filters, reaching fainter flux sensitivity for line emission

TFI unique science example



Efficient detection of
first-light
Lyman alpha emitters

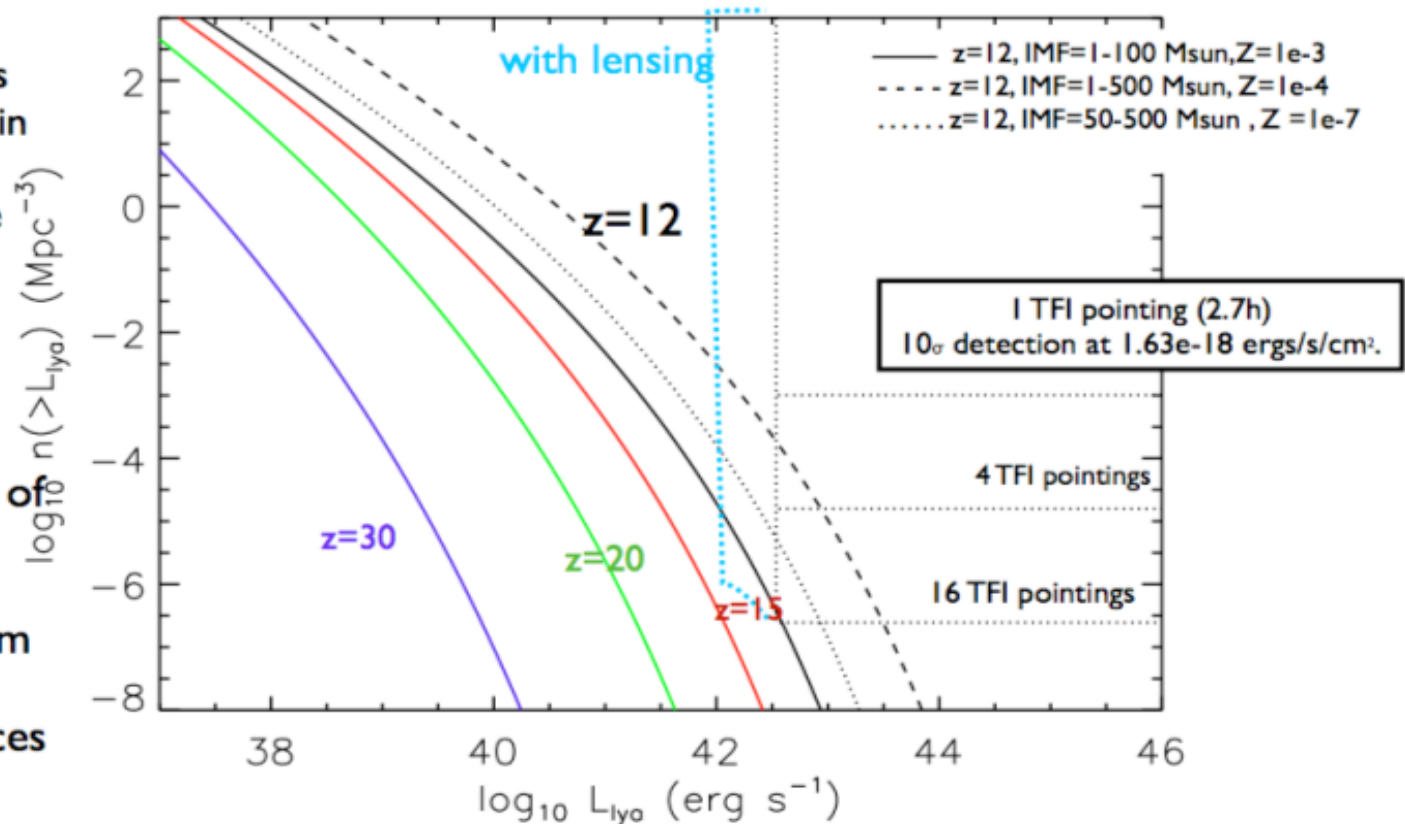


High-Redshift Science with TFI

- * Predictions of Lyman Alpha emitting galaxies at $z=12, 15, 30$ are highly speculative
- * Can make a guess by using the parameters (IMF, metallicity, photon escape fraction) defined by population of LAEs at $z=6.5$ Kashikawa et al (2006)
- * However, **THIS IS EXPLORATORY SCIENCE**, TFI is the *best* and if the sources of *First Light* are very faint, it may be the *only* option

- * A single 2.7 hour pointing is sufficient to detect an LAE in the more optimistic, but plausible scenarios. Multiple pointings probe more volume and lead to higher possible detections.

- * Can 'tune' TFI to redshifts of suspected galaxy overdensities soon to be predicted from high- z 21 cm mapping of neutral hydrogen, increasing chances even more.





TFI can map the ionisation bubble evolution



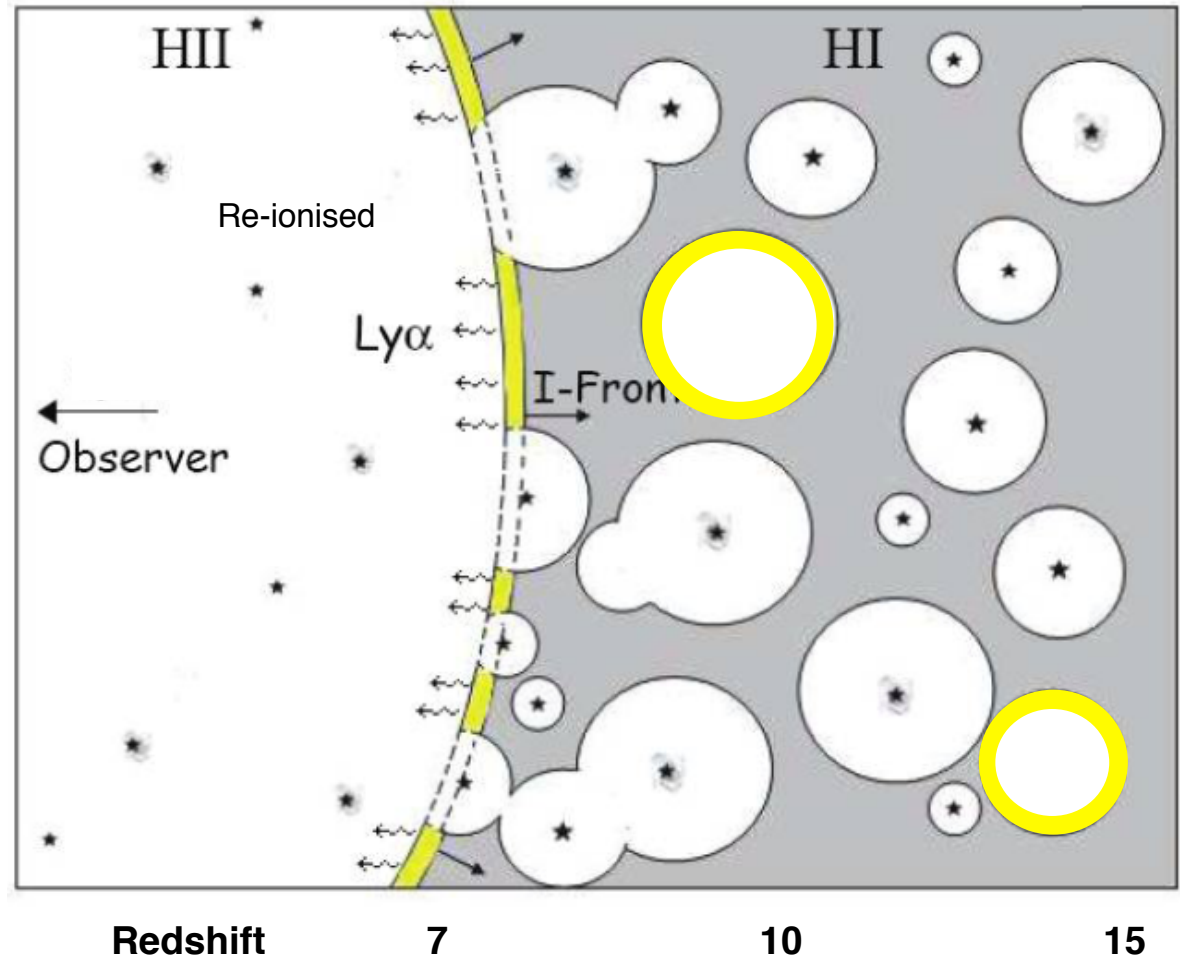
MAPPING NEUTRAL HYDROGEN DURING REIONIZATION WITH THE $\text{Ly}\alpha$ EMISSION FROM QUASAR IONIZATION FRONTS

SEBASTIANO CANTALUPO, CRISTIANO PORCIANI, AND SIMON J. LILLY

Ly alpha emission from bubble boundaries

Scanning through wavelengths (redshift) maps bubble sizes and density through reionisation Epoch

Sizes should match TFI field at $z > 10$

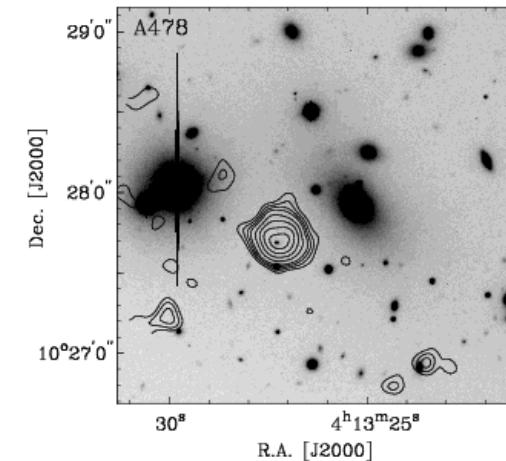


Example Object

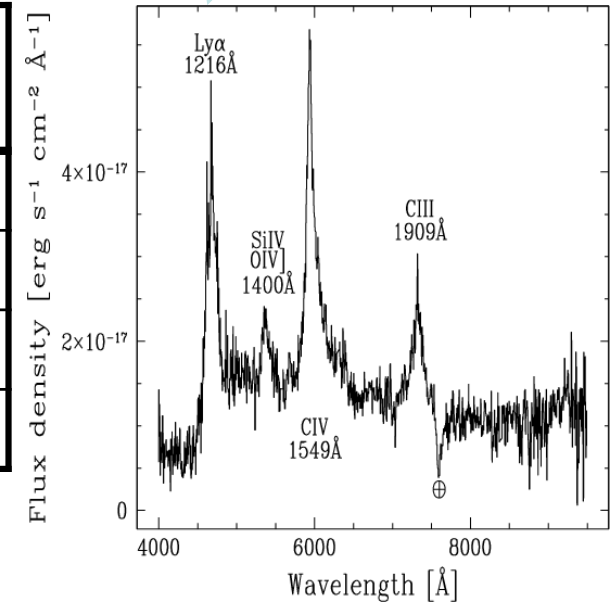


- A dusty quasar in the field of cluster Abell 478
- Discovered by its large sub-mm emission
- Redshift ~ 2.8 from Keck spectroscopy
- Gravitational lens effects are small ($\sim 1.3x$)
- Scaling this object to other redshifts gives:

Knudsen et al - Astroph/0308438



Redshift	CIV Emission Line		FGS-TF Sensitivity (10s in 10,000 s)
	wavelength	Flux (W / m^2)	
2.8	0.6 μm	4.6×10^{-18}	-
7.0	1.24 μm	2.3×10^{-20}	1.0×10^{-20}
15.0	2.48 μm	1.5×10^{-20}	3.5×10^{-21}
20.0	3.26 μm	4.9×10^{-21}	2.8×10^{-21}





Thank you

This lecture was funded in part by the Marie Curie Initial Training Network ELIXIR of the European Commission under contract PITN-GA-2008-214227.